
FORECASTING WITH HYPER-TREES

Alexander März *

Kashif Rasul

ABSTRACT

We introduce the concept of Hyper-Trees and offer a new direction in applying tree-based models to time series data. Unlike conventional applications of decision trees that forecast time series directly, Hyper-Trees are designed to learn the parameters of time series models. Our framework combines the effectiveness of gradient boosted trees on tabular data with the advantages of established time series models, thereby naturally inducing a time series inductive bias to tree models. By relating the parameters of a target time series model to features, Hyper-Trees also address the issue of parameter non-stationarity. To resolve the inherent scaling issue of boosted trees when estimating a large number of target model parameters, we combine decision trees and neural networks within a unified framework. In this novel approach, the trees first generate informative representations from the input features, which a shallow network then maps to the target model parameters. With our research, we aim to explore the effectiveness of Hyper-Trees across various forecasting scenarios and to extend the application of gradient boosted trees outside their conventional use in time series modeling.

Keywords Forecasting · Gradient Boosting Machines · Hyper-Networks · Parameter Non-Stationarity · Time Series

1 Introduction

Gradient boosted decision trees (GBDTs) (Friedman, 2001) are widely recognized for their accuracy in both regression and classification tasks, while also offering efficient scalability for large datasets. Transitioning from their original design as general-purpose tree models, frameworks such as LightGBM (Ke et al., 2017) have lately also gained prominence in the forecasting domain, demonstrating excellent performance in competitions like the M5 (Makridakis et al., 2022a,b). In an extensive overview, Januschowski et al. (2022) attribute the success of GBDTs within a time series context to several factors. Key among these are their robustness, relative insensitivity to hyper-parameters, and versatility in handling numerical and categorical features. Further, GBDTs are effective at capturing complex non-linear relationships and interactions, as well as their adaptability to diverse time series characteristics. These attributes position tree-based models as competitive, out-of-the-box forecasting tools for effective use across a wide range of time series applications.

Besides their advantages, however, general purpose tree-based models are not designed to handle sequential data naturally, which presents a significant limitation in forecasting applications (Godahewa et al., 2023). Unlike time series models, like ARIMA (Box et al., 2015), Exponential Smoothing (Holt, 1957; Winters, 1960) or recurrent neural networks (RNNs) and their variants, e.g., LSTMs (Hochreiter and Schmidhuber, 1997) or GRUs (Cho et al., 2014), GBDTs struggle to recognize and account for the sequential order and temporal dependencies inherent in time series data. These limitations usually necessitate careful feature engineering to embed time series information effectively, e.g., via adding lagged or rolling features derived from the target to be forecasted (Sprangers et al., 2023; Nasios and Vogklis, 2022). More importantly, since most GBDTs provide a piece-wise constant in the leaf nodes, standard implementations of tree-based models are not adept at forecasting beyond the range of the data they have been trained on (Godahewa et al., 2023). A commonly adopted strategy for addressing some of these limitations involves first removing seasonality and trend from the series and then fitting a GBDT to the residuals. The final forecast is then composed of two parts: a local model that forecasts trend and seasonality, e.g., ARIMA (Box et al., 2015), and a tree-based forecast. However, this approach has its own set of challenges. It is less suited for series that lack clear trends or seasonality, becomes complex to maintain for large-scale forecasting applications involving numerous time series, and prevents leveraging cross-series information since separate models are applied for modeling local trend and seasonality. To better adapt

* Author for correspondence: alex.maerz@gmx.net

tree-based models to a time series domain, several approaches have in response been proposed in the literature. Notable contributions include those of [Shi et al. \(2019\)](#) and [de Vito \(2017\)](#), who enhance tree structures by replacing piece-wise constant trees with piece-wise linear trees. This adaptation enables tree-based forecasts to extend beyond the training data range, overcoming the limitations of conventional piece-wise constant trees. Building on the relationship between threshold autoregressive models and decision trees, [Godaheva et al. \(2023\)](#) introduce a specialized tree algorithm for forecasting. Their approach employs time series-specific splitting and stopping procedures while training global pooled regression models in the leaves to leverage cross-series information.

These advancements have markedly improved the ability of GBDTs to better adapt to a time series context. Nevertheless, effective modeling of temporal dynamics within a GBDT framework presents ongoing challenges and remains an active area of research. To further progress in this domain, we propose a novel approach that extends tree-based models more naturally to a time series context via the use of Hyper-Trees. Unlike conventional tree-based approaches that model and forecast time series directly, Hyper-Trees focus on learning parameters of a wide class of target time series models. By reformulating GBDTs into a Hyper-Tree architecture, we combine the benefits of tree-based modeling with the inductive bias of time series models. To the best of our knowledge, we are among the first to transfer the concept of hyper-models to GBDTs. While our approach is built upon the well-established LightGBM model ([Ke et al., 2017](#)), our framework can in principle be applied to any modern GBDT algorithm. In the following, we detail the advantages of using Hyper-Trees for time series modeling and forecasting:

- **Enhanced Forecasting Capability** Hyper-Trees offer a distinct advantage in forecasting compared to standard GBDTs. Traditional GBDTs typically provide piece-wise constant values in the leaf nodes, which constrains their forecasts to the value range observed in the training set ([Godaheva et al., 2023](#)). This limitation makes it challenging for GBDTs to extrapolate or model trends effectively. While LightGBM ([Ke et al., 2017](#)) allows to fit linear ([Shi et al., 2019](#)) rather than piece-wise constant trees to partially address this issue, other GBDT implementations lack this functionality. In contrast, Hyper-Trees generate forecasts through a two-step process: first, they forecast the parameters of the target model. Then, these parameters are applied to the target model to produce the final forecast. This approach allows Hyper-Trees to leverage the inductive bias of the target models, enabling them to generate forecasts that can naturally extend beyond the value range of the train data. This capability is crucial for any forecasting task, particularly for time series exhibiting strong trends or multiplicative seasonality.
- **Cross-Series Learning with Local Adaptivity** In the evolving landscape of time series modeling, Hyper-Trees have the potential to redefine the use of local forecasting models. Classical local methods like ARIMA ([Box et al., 2015](#)) or Exponential Smoothing ([Holt, 1957](#); [Winters, 1960](#)) typically require individual model training for each time series. For instance, in forecasting sales data across various regions, conventional practices would necessitate a distinct model for each region, a process that, while ensuring specificity, does not leverage cross-series information. Hyper-Trees, in contrast, combine global learning with local adaptivity. Instead of treating each time series in isolation, they learn the parameters of a target model across all series. In the sales data scenario, a Hyper-Tree would model all regions collectively, identifying common patterns and trends. It then provides model parameters for each region-specific model. Hence, Hyper-Trees allow for parameter sharing across different series, enhancing the stability of model training and forecasting. At the same time, they maintain the local adaptivity necessary for accurate forecasts for each series.
- **Time-Varying Parameter Estimation** Hyper-Trees bring a dynamic approach to parameter estimation, diverging from the static nature of model parameters. Unlike conventional training and forecasting of time series models, where a set of parameters is estimated that remains fixed for the test set, Hyper-Trees generate parameter forecasts at an observational level. For each time step in the test set, they forecast the target model parameters, allowing for adaptability as new information becomes available. This dynamic parameterization enables Hyper-Trees to efficiently respond to a non-stationary environment commonly present in time series data, without the need for model re-training ([Lee et al., 2023](#)).
- **Advanced Optimization and Structural Constraints** Hyper-Trees also offer an advantage in model training by utilizing a more comprehensive approach to parameter estimation. Unlike conventional optimization that mostly relies on first order approximation of the loss function, Hyper-Trees incorporate both gradients and the Hessian, enabling more efficient parameter updates. Compared to estimating classical linear time series models, Hyper-Trees further offer the advantage of modeling non-linear relationships and interactions between features, enabling them to capture complex patterns in the parameters. Moreover, Hyper-Trees make it conceptually easy to impose structural assumptions on estimated parameters that allows modeling of, e.g., strictly increasing or decreasing time series patterns. Such assumptions can be imposed by leveraging GBDTs' monotonicity constraints or by manually adding restrictions on the estimated parameters. This ensures that the estimated parameters adhere to predefined behaviors and align forecasts with expected real-world patterns.

To maintain the scalability of our approach in situations that require estimating a large number of target model parameters, we propose a hybrid architecture that unifies GBDTs and neural networks within a single framework. This approach preserves the strong feature learning capabilities of GBDTs for tabular data while exploiting the efficiency of neural networks in modeling multi-output tasks. Traditionally, GBDTs use a one-vs-all strategy, estimating one tree per parameter, which can be computationally expensive since it scales almost linearly with the number of parameters (Iosipoi and Vakhrushev, 2022). In contrast, our hybrid model utilizes GBDTs to first generate informative representations from the input features which serve as input to a shallow neural network that maps to the target model parameters. We keep the GBDT embedding dimension low to maintain a tractable runtime. To compensate for this and enhance the neural network’s learning capacity, we expand the tree embeddings into a higher-dimensional space using random projection matrices. This expansion diversifies the representations and increases the input dimensions for the subsequent neural network. Recent studies have shown that incorporating random projection matrices can improve the accuracy of both GBDTs and deep learning models without increasing computational complexity, which motivates their use in our approach (Yeh et al., 2024; Iosipoi and Vakhrushev, 2022; Casale et al., 2011). Subsequently, a shallow neural network, such as a Multi-Layer Perceptron (MLP), maps the projected representations to the final target model parameters. It is important to note that both the GBDTs and the MLP are trained jointly, rather than in a two-step procedure. This contrasts with most existing approaches where the GBDTs are trained first and then the neural network is trained separately. Joint learning enables the GBDTs and the neural network to optimize together, leading to improved performance by fully leveraging the interplay between feature learning and parameter mapping. Our approach seamlessly combines GBDTs with neural networks, all within the familiar syntax and code of established GBDTs frameworks. This allows for easy customization of the network architecture, enabling researchers and practitioners to adapt the framework to specific problem domains.

The remainder of this paper is organized as follows: Section 2 introduces the concept of Hyper-Trees and describes their integration into different model classes. Section 3 gives an overview of related works, while Section 4 presents the application of Hyper-Trees across various datasets and applications. Finally, Section 5 concludes. We hope that our exploration of Hyper-Trees not only serves as a starting point to inspire future research and development in this field but also initiates a broader discussion about the potential of tree-based models beyond their conventional use in time series analysis and forecasting.

2 Hyper-Trees

Hyper-networks, introduced by Ha et al. (2017), have emerged as a valuable concept in machine learning. These networks are designed to generate parameters for a target network, with their key feature being that the generated parameters are modeled as functions of input features. The integration of hyper-networks has proven to be a significant advancement in the field, offering new possibilities for adaptive and context-dependent modeling. Such integration enables the target network to adapt more seamlessly to changes in data patterns, without the need to retrain the target model. The dual-level modeling approach, where the hyper-network customizes the target network’s parameters in response to an evolving environment, ensures that the learning process is highly adaptive.

While hyper-models have shown great potential, they have primarily been explored within the realm of deep learning. In this paper, we extend this concept beyond neural networks to GBDTs. We term our framework Hyper-Trees, drawing a parallel to hyper-networks. Just as hyper-networks generate parameters for a target network, our Hyper-Trees learn to generate parameters for a target time series model. The gradient-based nature of GBDTs allows the target model to be a member of a wide class of time series models, e.g., ARIMA (Box et al., 2015), Exponential Smoothing (Holt, 1957; Winters, 1960), as well as other target model architectures. By training the Hyper-Tree and applying the learned parameters to the target model in a unified framework, our approach flexibly and efficiently incorporates time series inductive biases without changing the implementation of the most commonly used GBDTs. Compared to hyper-networks which often require extensive data and which are more likely to over-fit, modeling parameters of a target model via Hyper-Trees provides a more efficient and robust approach, especially in scenarios with limited data availability, which are common in real-world applications (Bansal et al., 2022; Vogelsgesang et al., 2018). Our Hyper-Tree approach is designed and expected to perform well on complex, operational time series data (Januschowski and Kolassa, 2019) where global tree-based models typically excel, i.e., sparse datasets with missing values and high-dimensional feature sets that extend beyond basic time series information, including sales campaigns, calendar events and categorical meta-features. By modeling the parameters of a target model, our approach aims to be both modular and accurate by combining the efficacy of tree-based models with the inductive bias of time series models. In the following, we explain the concept of Hyper-Trees in more detail.

2.1 Gradient Boosted Decision Trees

We briefly review the workings of GBDTs, since this is crucial for introducing the concept of Hyper-Trees. This section is general enough so that commonly used GBDTs, such as LightGBM (Ke et al., 2017) or XGBoost (Chen and Guestrin, 2016) are special cases. In its most general formulation, the estimation of GBDTs at each iteration m is based on minimizing a regularized objective function

$$\mathcal{L}^{(m)} = \sum_{i=1}^N \ell[y_i, \hat{y}_i^{(m-1)} + f_m(\mathbf{x}_i)] + \Omega(f_m), \quad (1)$$

where ℓ is a differentiable convex loss function that measures the discrepancy between the model estimates of the i -th instance at the m -th iteration $\hat{y}_i^{(m)} = \hat{y}_i^{(m-1)} + f_m(\mathbf{x}_i)$ and the true value y_i , while $\Omega(\cdot)$ is a regularization term that penalizes the complexity of the model to avoid over-fitting. A second order approximation of $\ell[\cdot]$ and dropping constant terms allows us to re-write Equation (1) as follows

$$\mathcal{L}^{(m)} = \sum_{j=1}^T [G_j w_j + \frac{1}{2}(H_j + \lambda)w_j^2] + \gamma T, \quad (2)$$

where $G_j = \sum_{i \in I_j} g_i$, $H_j = \sum_{i \in I_j} h_i$, $g_i = \partial_{\hat{y}_i^{(m-1)}} \ell[y_i, \hat{y}_i^{(m-1)}]$ and $h_i = \partial_{\hat{y}_i^{(m-1)}}^2 \ell[y_i, \hat{y}_i^{(m-1)}]$ are first and second order derivatives, $I_j = \{i | q(x_i) = j\}$ is the set of indices of data points assigned to the j -th leaf, γ is a parameter that controls the penalization for the number of terminal nodes T of the trees, and λ is a L_2 regularization term on the leaf weights w_j . For a fixed tree structure, the optimal weight w_j^* of leaf j can be obtained by

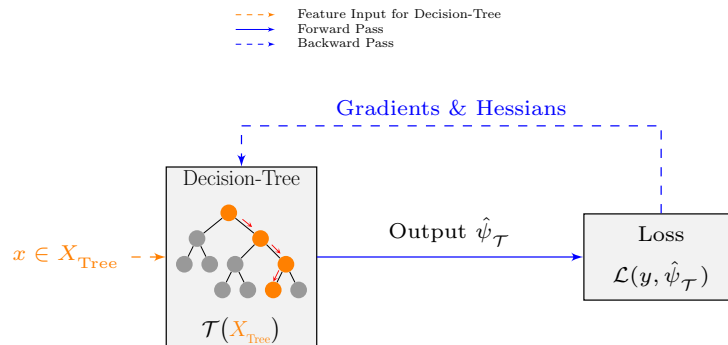
$$w_j^* = \frac{G_j}{H_j + \lambda}. \quad (3)$$

Using w_j^* and reformulating Equation (2), the objective function is given as follows

$$\mathcal{L}^* = -\frac{1}{2} \sum_{j=1}^T \frac{G_j^2}{H_j + \lambda} + \gamma T. \quad (4)$$

From Equation (4) it follows that, as long as gradients and Hessians are defined, any twice-differentiable function can be used. Since GBDTs rely on second-order derivatives, Equation (4) shows that GBDTs work as Newton-Raphson in function space (Sigrist, 2021). To provide a clearer understanding, Figure 1 illustrates the typical workflow of GBDTs.

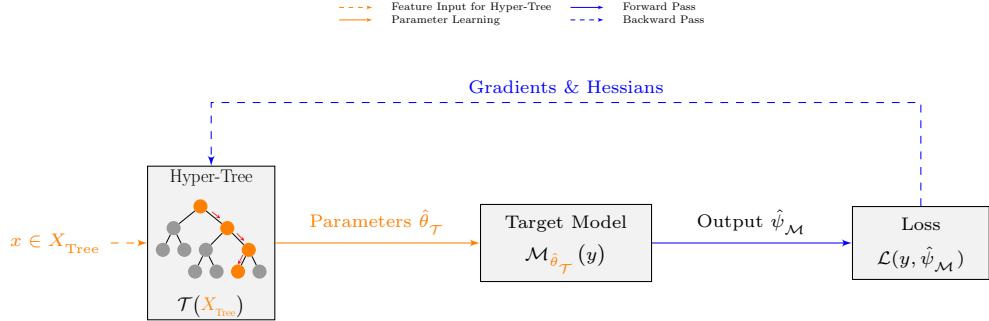
Figure 1: Typical GBDT architecture.



2.2 Hyper-Tree Architecture

The conventional use of GBDTs involves learning the output $\hat{\psi}_{\mathcal{T}}$ directly, with common choices for the loss function \mathcal{L} being Mean Squared Error (MSE) and its variants. However, according to Equation (4), GBDTs can utilize any twice-differentiable loss function for model training. As such, as long as the gradients and Hessians are defined, GBDTs can be extended to the concept of Hyper-Trees that learn the parameters of a target model. By conceptualizing GBDTs as Hyper-Trees, we perform gradient descent in parameter space, diverging from the conventional tree-based methods that operate in function space. The architectural design and process flow are depicted in Figure 2.

Figure 2: Hyper-Tree architecture.



The architecture in Figure 2 shows a unified and modular framework, with the Hyper-Tree as the central component. The Hyper-Tree takes a set of input features X_{Tree} and generates parameters $\hat{\theta}_{\mathcal{T}}$ that are used by the target model \mathcal{M} . The target model then creates an output $\hat{\psi}_{\mathcal{M}}$ which is subsequently used as input in a shared loss function \mathcal{L} . The loss function, guided by both the Hyper-Tree and the target model, integrates their outputs to derive gradients and Hessians. This ensures that the loss calculation captures the dynamics of both the Hyper-Tree structure and the target model's behavior, reflecting the interplay between both components. For the architecture shown in Figure 2, the temporal component can be modeled via, e.g., an AR(p)-process, although the target model can be any type of time series model. The input X_{Tree} would include a diverse range of categorical and numerical features. Contrary to time series models that learn directly from data, the target model in this framework does not. Instead, its role is to induce a specific inductive bias as well as temporal dependencies to the Hyper-Tree. Via gradients and Hessians that are derived from the shared loss function, this bias guides the Hyper-Tree to capture and model the temporal dependencies present in the data by generating parameters $\hat{\theta}_{\mathcal{T}}$ that are specific to each time step, effectively encoding the temporal information into the parameters it generates. Consequently, in a Hyper-Tree setup, the target model acts more as a function applying the parameters generated by the Hyper-Tree, rather than learning and internalizing the temporal dependencies on its own. Based on the gradients and Hessians that are derived from the shared loss function, as well as from the input features it receives for each time step, the Hyper-Tree is the component that learns to encode these dependencies into the target model parameters. Figure 2 illustrates how the target model influences the learning process of the Hyper-Tree, ensuring that the temporal aspects of the data are incorporated. By reformulating well-established GBDTs into a Hyper-Tree architecture, we combine the benefits of tree-based learning of the target-model parameters with the inductive bias of a wide variety of time series models, thereby extending GBDTs to a time series context more naturally. The combination of tree-based learning and target model inductive bias allows for more dynamic forecasting capabilities compared to conventional tree-based models. Notably, forecasts of the Hyper-Tree are capable of exhibiting trend growth, which sets them apart from conventional GBDTs models. This difference arises from the fact that Hyper-Tree forecasts are generated through the inductive bias of the target models. In classical GBDTs, forecasts are typically piecewise constant and constrained to the value range of the train-set. In contrast, Hyper-Tree models forecast parameters of a target model, rather than direct outputs. This approach allows the resulting forecasts to naturally extend beyond the training set's range. By operating in the parameter space, Hyper-Tree models can produce meaningful forecasts even for previously unseen values, overcoming a key limitation of conventional GBDTs.

Besides the architectural design shown in Figure 2, the modularity of our approach allows the framework to be extended to a probabilistic setting, where instead of $\hat{\psi}_{\mathcal{M}}$ being a point-forecast, the Hyper-Tree architecture can be used to model and forecast parameters of a distribution, from which forecast intervals and quantiles of interest can be derived.² In

²For recent extensions of tree-based models to a probabilistic setting, we refer the interested reader to März and Kneib (2022); März (2022, 2019); Sprangers et al. (2021); Hasson et al. (2021); Duan et al. (2020).

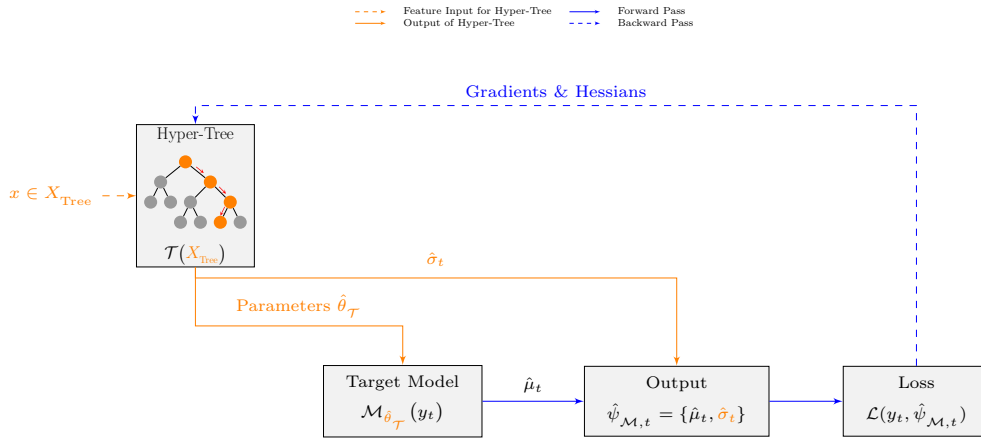
general, any suitable distribution that characterizes the data can be specified. As an example, one can assume a Normal distribution $y_t \sim N(\mu_t, \sigma_t)$, where the mean and standard deviation are parameterized as follows

$$\mu_t = \theta_{1,t}(\mathbf{x}_t)y_{t-1} + \theta_{2,t}(\mathbf{x}_t)y_{t-2} + \dots + \theta_{p,t}(\mathbf{x}_t)y_{t-p}, \quad (5)$$

$$\sigma_t = \text{softplus}(\theta_{\sigma,t}(\mathbf{x}_t)). \quad (6)$$

In this example, we parameterize μ_t via an AR(p) model. Even though we can in principle impose structural assumptions for σ_t as well, e.g., ARCH/GARCH models (Engle, 1982; Bollerslev, 1986), one can directly estimate σ_t via the Hyper-Tree as illustrated in Figure 3.

Figure 3: Distributional Hyper-Tree Architecture.



Instead of modeling parameters of a distribution, creating probabilistic forecasts via conformal predictive distributions (Vovk et al., 2022; Johansson et al., 2023) or conformalized quantile regression (Romano et al., 2019) present interesting alternatives. However, in this study, we restrict our focus to point forecasts, leaving the exploration of probabilistic extensions for future research. Due to its modularity, where both the Hyper-Tree and the target model can be interchangeably replaced or modified as required by the specific characteristics of the data, gradients and Hessians typically do not have an analytical solution. We therefore leverage the automatic differentiation capabilities as available in PyTorch (Paszke et al., 2019) for deriving gradients and Hessians.

3 Related Work

Recent advancements in the application of Hyper-Networks have yielded significant contributions across various fields, reflecting an increasing interest. In the area of time series forecasting, Lee et al. (2023) propose HyperGPA, a hyper-network designed to address the challenges of temporal drifts in time series data by generating optimal model parameters for each period. By leveraging computational graph structures, HyperGPA achieves up to a 64.1% improvement in forecasting accuracy compared to baselines. Duan et al. (2022) introduce Hyper Time Series Forecasting (HTSF), a hyper-network-based framework that tackles distribution shift problems in time series forecasting. HTSF jointly learns time-varying distributions and corresponding forecasting models, demonstrating state-of-the-art performance on several benchmarks. Fons et al. (2022) explore the use of hyper-networks in Implicit Neural Representations (INRs) for time series data representation and analysis. Their work demonstrates the potential of INRs in time series imputation and generative tasks, showcasing competitive performance against existing approaches. Combining state space models with deep learning for probabilistic time series forecasting, Rangapuram et al. (2018) parameterize a per-time series linear state space model with a recurrent neural network, balancing data efficiency and interpretability with the ability to learn complex patterns from raw data. In their paper, Medeiros and Veiga (2000) introduce a neural coefficient smooth transition autoregressive model for nonlinear time series analysis and forecasting. By incorporating a neural network to control time-varying parameters, their model offers advantages over traditional approaches, including the incorporation of linear multivariate thresholds and smooth transitions between regimes. To leverage the strengths of both modeling frameworks, there has been a growing interest in hybrid models that blend tree-based methods with neural networks. In their approaches, Karingula et al. (2022) and Badirli et al. (2020) develop variants of gradient boosting that use deep neural networks as weak learners. In a parallel line of research, Emami and Martínez-Muñoz (2022) explore

training the final layers of a neural network using gradient boosting principles, whereas [Kontschieder et al. \(2016\)](#) propose integrating differentiable decision trees into neural networks for end-to-end training. Extending on the work of [Prokhorenkova et al. \(2018\)](#), [Popov et al. \(2020\)](#) introduce NODE, a deep learning architecture designed for tabular data that generalizes ensembles of oblivious decision trees while leveraging end-to-end gradient-based optimization and multi-layer hierarchical representation learning. In particular, the NODE architecture of [Popov et al. \(2020\)](#) extends CatBoost ([Prokhorenkova et al., 2018](#)) by making decision trees differentiable, allowing for its integration into existing deep learning frameworks and enabling multi-layer architectures akin to end-to-end trained deep GBDTs. Related to this is the approach of [Horrell \(2024\)](#) that implements GBDTs as layers within the PyTorch framework of [Paszke et al. \(2019\)](#). For a more exhaustive overview on combining GBDTs with deep learning, we refer to [Li et al. \(2023\)](#).

4 Applications and Experiments

For our experiments, we use the following commonly used publicly available datasets:

- **Air Passengers:** This dataset contains the monthly totals of international airline passengers and is taken from [Alexandrov et al. \(2020\)](#); [Athanasopoulos et al. \(2011\)](#).
- **Australian Electricity Demand:** This dataset comprises five time series, each representing the electricity demand for five Australian states and is borrowed from [Godaheva et al. \(2021\)](#). Originally recorded at 30-minute intervals, we aggregate the data to a monthly time granularity for our analysis.
- **Australian Retail Turnover:** This dataset consists of a total of 133 monthly series and is borrowed from [O’Hara-Wild et al. \(2022\)](#).
- **M3 Monthly:** This dataset comprises 1,428 monthly time series, belonging to six distinct domains: demographic, microeconomic, macroeconomic, industry, finance, and other miscellaneous categories and is borrowed from [Makridakis and Hibon \(2000\)](#); [Godaheva et al. \(2021\)](#).
- **M5:** This dataset comprises daily sales records from Walmart, the world’s largest retailer by revenue. It encompasses 3,049 products across multiple stores and states, resulting in 42,840 distinct time series due to its multi-level hierarchical structure ([Makridakis et al., 2022a,b](#)). We aggregate the data to the store-department level, yielding 70 daily time series. This aggregation is motivated primarily to reduce the intermittency present at the most granular level of the data.
- **Rossmann Store Sales:** This dataset consists of a total of 1,115 daily series and is borrowed from [Knauer and Cukierski \(2015\)](#). We subset the data to include stores that are open ($Open = 1$).
- **Tourism:** This dataset consists of a total of 366 monthly series and is borrowed from [Alexandrov et al. \(2020\)](#); [Athanasopoulos et al. \(2011\)](#).

As references, we compare our Hyper-Trees to the following models:

- **AR(p):** An autoregressive model with p lags.
- **AR(p)-X:** same as AR(p) with additional features.
- **Auto-Arima:** an ARIMA ([Box et al., 2015](#)) model where optimal $(p, d, q)(P, D, Q)$ are selected.
- **Auto-Arima-X:** same as Auto-Arima with additional features.
- **Auto-ETS:** an Exponential Smoothing ([Holt, 1957](#); [Winters, 1960](#)) model, where the model specification is selected automatically.
- **Chronos:** Chronos is a family of pre-trained time series forecasting models based on language model architectures ([Ansari et al., 2024](#)). For all experiments, we use the chronos-t5-base version.
- **Deep-AR:** A probabilistic forecasting model that uses autoregressive recurrent neural networks ([Salinas et al., 2020](#)).
- **LightGBM:** LightGBM model of [Ke et al. \(2017\)](#).
- **LightGBM-AR(p):** Same as LightGBM with additional autoregressive lagged-target features of order p .
- **LightGBM-STL:** Each series is first de-trended and de-seasonalized via a cubic polynomial. The remainder is then modeled via a local LightGBM ([Ke et al., 2017](#)) model.
- **Temporal Fusion Transformer (TFT):** An attention-based architecture for multi-horizon time series forecasting ([Lim et al., 2021](#)).

Classical time series models are trained locally and evaluated on datasets where time-derived features only are available. Due to their cross-learning capabilities, as well as their ability to incorporate a richer feature set including categorical and numeric variables alongside temporal information, deep learning-based models are used for global model training and evaluation. All local forecasting models are estimated using the Nixtla-implementation of [Garza et al. \(2022\)](#), whereas the deep-learning models are estimated via the implementations available in GluonTS of [Alexandrov et al. \(2020\)](#); [Athanasopoulos et al. \(2011\)](#). The LightGBM-STL model is estimated using the sktime implementation of [Király et al., 2024](#); [Löning et al., 2019](#)). To ensure a practical comparison across global models, we standardized hyper-parameters as much as possible across all models for each specific dataset. Our decision to forgo hyper-parameter optimization mimics real-world scenarios where exhaustive hyper-parameter optimization may not always be feasible due to time or computational constraints. For details on the hyper-parameters, see Tables [B1](#) and [B2](#). Also, it is worth emphasizing that none of the Hyper-Tree models incorporate lagged target values as features. For our experiments, we start with a simple illustrative example in Section [4.1](#) and continue with an evaluation across multiple datasets in Sections [4.2](#) and [4.3](#). Owing to its proven accuracy and popularity in the time series community, we use LightGBM ([Ke et al., 2017](#)) as the GBDT backbone for our Hyper-Tree models across all experiments.

4.1 Local Time Series Model: Introductory Example

We start our analysis with the Air Passengers dataset, as available in [Alexandrov et al. \(2020\)](#), which consists of monthly totals of airline passengers from 1949 to 1960. It is a popular dataset in time series forecasting and its trend and seasonality characteristics make it particularly suitable for the ARIMA ([Box et al., 2015](#)) to be a strong baseline. We split the data into train and test, where the last year is used as a hold-out set. The first step for analyzing such a time series dataset is typically a decomposition into seasonality, trend, and remainder. This STL decomposition is usually done via a LOESS-based estimation of each component ([Cleveland et al., 1990](#)). However, in the following, we use our Hyper-Tree architecture for decomposing the train series. The Hyper-Tree-STL parameterizes the following trend and seasonality components

$$\text{Trend}_t = \theta_{0,t}(\mathbf{x}_t) + \theta_{1,t}(\mathbf{x}_t) \cdot t \quad (7)$$

$$\text{Seasonality}_t = \sum_{i=1}^{N_{\text{season}}} \left(\theta_{\text{sin}_{i,t}}(\mathbf{x}_t) \cdot \sin \left(t \cdot i \cdot \frac{2\pi}{p} \right) + \theta_{\text{cos}_{i,t}}(\mathbf{x}_t) \cdot \cos \left(t \cdot i \cdot \frac{2\pi}{p} \right) \right) \quad (8)$$

where the parameters $\Theta_{\mathcal{T}}(\mathbf{x}_t) = [\theta_{0,t}(\mathbf{x}_t), \theta_{1,t}(\mathbf{x}_t), \theta_{\text{sin}_{i,t}}(\mathbf{x}_t), \theta_{\text{cos}_{i,t}}(\mathbf{x}_t)]$ are modeled as functions of time-derived features $\mathbf{x}_t = \{\text{month}, \text{quarter}, \text{year}, \text{time}\}$, with *time* being a linearly increasing integer. Even though the trend part in Equation (7) is specified as a linear function of t , the interactions and non-linearities induced by the Hyper-Tree allow for modeling also complex non-linear patterns. To ensure the trend is a smooth function of time, we add a term that penalizes squared first and second order differences, thereby encouraging neighboring estimates to be close to each other. We represent the seasonality via periodic Fourier-terms that are composed of multiple sine and cosine components, each with different frequencies and amplitudes, where $\theta_{\text{sin}_{i,t}}(\mathbf{x}_t)$ and $\theta_{\text{cos}_{i,t}}(\mathbf{x}_t)$ represent the sine and cosine weights for the i -th seasonal component. For Hyper-Tree-STL, we set $N_{\text{season}} = 1$ and $p = 12$ since the data is recorded on a monthly frequency. Instead of tuning the hyper-parameters, we use the default values and train the model for 500 iterations using the MSE as the loss function with the learning rate set to $\eta = 0.1$. Figure 4 shows the trend and seasonality estimated on the training dataset. As a reference, we add the components of a conventional STL decomposition as available in [Seabold and Perktold \(2010\)](#).

Figure 4: STL Decomposition.

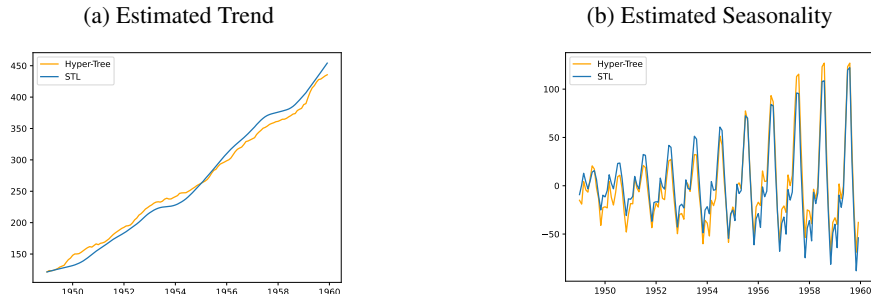
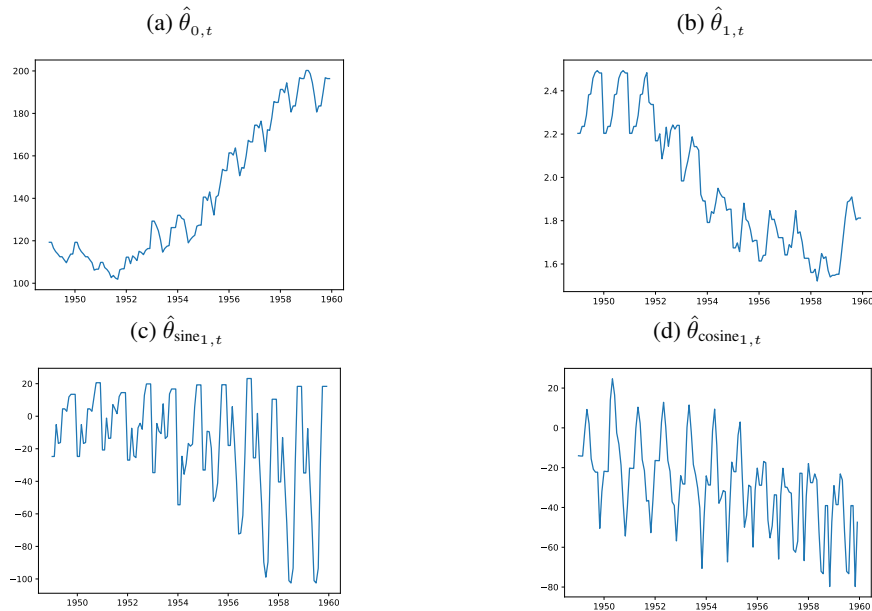


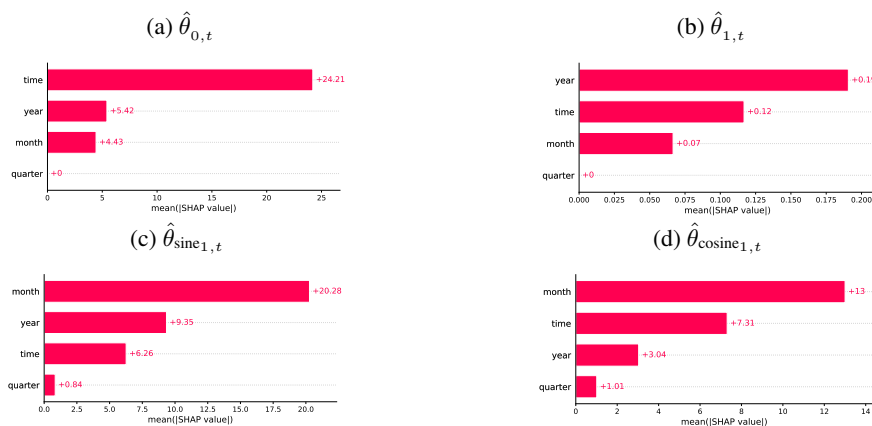
Figure 4 shows that the STL components estimated via the Hyper-Tree-STL and the traditional LOESS-based decomposition are in close agreement, even though the trend-estimate of the Hyper-Tree-STL is not as smooth. Considering the current use of relatively simplistic elements for estimating trend and seasonality, their approximation quality could possibly be enhanced by using more complex target models, e.g., via a penalized spline approach (Wood, 2017). In terms of model interpretability, we can investigate the estimated parameters over time, as illustrated in Figure 5.

Figure 5: Estimated STL Parameters.



Panels 5a and 5b show how the intercept and slope parameters vary over time, while Panels 5c and 5d depict the seasonality patterns of the estimated parameters. Besides the estimated parameters, we also have access to SHAP values (Lundberg et al., 2020; Lundberg and Lee, 2017) and feature importances for each estimated parameter, further increasing model interpretability.

Figure 6: Feature Importance of STL Parameters.



The feature importances for the trend parameters (Panels 6a and 6b) show that mostly features related to the progression of time $\{year, time\}$ are considered important, while the $\{month\}$ feature that reflects the within year patterns ranks highest for the seasonality parameters (Panels 6c and 6d). From the above STL discussion, we can infer that our Hyper-Tree-STL approach gives very close results to the conventional decomposition, with the added benefit of model and parameter interpretability. As the second step of our analysis, we now turn to the forecasting part for the last 12 months of the Air Passengers dataset. As target models, we specify the following Hyper-Tree-AR(12) model

$$y_t = \phi_{1,t}(\mathbf{x}_t)y_{t-1} + \phi_{2,t}(\mathbf{x}_t)y_{t-2} + \dots + \phi_{12,t}(\mathbf{x}_t)y_{t-12} \quad (9)$$

with time-step and feature specific parameters $\{\phi_{1,t}(\mathbf{x}_t), \dots, \phi_{12,t}(\mathbf{x}_t)\}$, as well as an Hyper-Tree-ES model with a damped trend and multiplicative seasonality (Hyndman and Athanasopoulos, 2021)

$$\begin{aligned} \ell_t &= \alpha_t(\mathbf{x}_t)(y_t/s_{t-m}) + (1 - \alpha_t(\mathbf{x}_t))(\ell_{t-1} + \phi_t(\mathbf{x}_t)b_{t-1}) \\ b_t &= \beta_t(\mathbf{x}_t)(\ell_t - \ell_{t-1}) + (1 - \beta_t(\mathbf{x}_t))\phi_t(\mathbf{x}_t)b_{t-1} \\ s_t &= \gamma_t(\mathbf{x}_t)\frac{y_t}{(\ell_{t-1} + \phi_t(\mathbf{x}_t)b_{t-1})} + (1 - \gamma_t(\mathbf{x}_t))s_{t-m} \end{aligned} \quad (10)$$

with the h-step ahead forecast given by

$$\hat{y}_{t+h|t} = \left[\ell_t + (\phi_{t+1}(\mathbf{x}_{t+1}) + \phi_{t+2}^2(\mathbf{x}_{t+2}) + \dots + \phi_{t+h}^h(\mathbf{x}_{t+h}))b_t \right] s_{t+h-m(k+1)}.$$

where $\{\ell_t, b_t, s_t\}$ denote $\{level, trend, seasonality\}$ with corresponding time-step and feature specific parameters $\{\alpha_t(\mathbf{x}_t), \beta_t(\mathbf{x}_t), \gamma_t(\mathbf{x}_t)\}$, m indicates the frequency of the seasonality and $\{\phi_t(\mathbf{x}_t), \dots, \phi_{t+h}(\mathbf{x}_{t+h})\}$ control the dampening of the trend. The choice of the target AR(12) model is not based on any automated model selection. Instead, the decision to use 12 lags stems from the monthly nature of the dataset. Similarly, the trend and seasonality of the Air Passengers dataset have led us to specify an Exponential Smoothing (Holt, 1957; Winters, 1960) model with multiplicative seasonality and damped trend, since this specification often provides accurate and robust forecasts (Hyndman and Athanasopoulos, 2021).

Table 1: Air Passengers Results.

Model	MAPE	sMAPE	WAPE	RMSE	MAE
AR	8.570	9.143	9.254	54.951	44.064
AR-X	8.745	9.335	9.377	55.172	44.652
Auto-Arima	4.188	4.039	3.896	23.955	18.551
Auto-Arima-X	3.559	3.593	3.682	21.161	17.533
Auto-ETS	4.499	4.589	4.677	25.280	22.270
Hyper-Tree-AR	2.506	2.454	2.383	15.557	11.346
Hyper-Tree-ES	3.411	3.418	3.192	20.520	15.201
LightGBM	2.830	2.804	2.710	15.366	12.905
LightGBM-AR	7.191	6.823	6.709	37.961	31.945
LightGBM-STL	3.993	4.041	4.147	24.303	19.746

Forecast-error metrics, lower is better. The best metrics are in bold. Mean Absolute Percentage Error (MAPE); Symmetric Mean Absolute Percentage Error (sMAPE); Weighted Absolute Percentage Error (WAPE); Root Mean Squared Error (RMSE); Mean Absolute Error (MAE).

Table 1 shows that the Hyper-Tree models are competitive, with the Hyper-Tree-AR being the most accurate across all metrics, except for RMSE, where LightGBM shows the highest accuracy. In contrast, while being the classical analog due to its architectural similarity to the Hyper-Tree-AR, the AR-X exhibits the lowest accuracy across all metrics. This underscores the significance of parameter learning and forecasting using a tree-based hyper-model, which distinguishes the Hyper-Tree-AR from AR-X. The Hyper-Tree-AR appears to more effectively capture the multiplicative behavior of the seasonal component of the series, likely due to its non-stationary AR-parameters that are forecasted as a function of time-related features and their interactions. Additionally, it is important to mention that while the Auto-Arima has been fine-tuned for the specific dataset - the selected model is an ARIMA(1, 1, 0)(0, 1, 0)[12] - the Hyper-Tree-AR is a plain AR(12) model without additional differencing or automated selection of lags. Hence, it is likely that the accuracy of the Hyper-Tree-AR can be further improved via, e.g., seasonal differencing and/or selecting a more appropriate lag structure. While the Hyper-Tree-ES compares well across metrics, it is not as competitive as the Hyper-Tree-AR. Yet, when compared to its classical analog, the Hyper-Tree-ES outperforms the Auto-ETS model across all metrics. The Hyper-Tree-ES also compares favorably well compared to the classical Auto-Arima and Auto-Arima-X models.

4.2 Local Time Series Models: Extended Evaluation

In the previous section, we applied and evaluated the Hyper-Tree architectures to a single, well behaved time series that exhibits strong seasonality and trend. As such, the repeating pattern of the series can easily be captured and modeled

using time derived features, leading to excellent forecasting results. To assess the performance of our Hyper-Tree architectures more comprehensively, we expand our evaluation to include additional datasets. The results of this extended analysis are presented in Table 2. It is important to note that we modify our approach for the Hyper-Tree-ES training for the Tourism dataset. This modification is driven by the computational demands of ETS model estimation, particularly for lengthy time series. The recursive nature of ETS estimation necessitates iterating over the entire series in each boosting step, substantially increasing runtime. This, combined with the estimation required for each series, makes local model estimation of our Hyper-Tree-ES computationally expensive for datasets with many series as available in the Tourism dataset. However, the ETS-type model offers a unique advantage in this context: unlike other models, the ETS offers the benefit of setting parameters manually, as the parameters are confined to values between 0 and 1. Leveraging this characteristic, we set parameters $\{\alpha_t, \beta_t, \gamma_t, \phi_t\}$ of Hyper-Tree-ES to a global value of 0.2 for each series in the Tourism dataset. A value of 0.2 generally results in a more conservative model that relies on historical patterns, resulting in smoother forecasts. We selected the optimal value by evaluating the accuracy over different values $\{0.1, \dots, 0.9\}$ on a hold-out set, using the average WAPE for selecting the optimal value.

Table 2: Local Model Results.

Dataset	Model	MAPE	sMAPE	WAPE	RMSE	MAE
Australian Electricity Demand	AR	60.272	8.202	6.950	480,701.7	280,845.7
	AR-X	60.496	8.125	6.877	478,058.1	278,627.4
	Auto-Arima	55.858	6.564	5.204	419,208.1	206,543.0
	Auto-Arima-X	62.278	9.450	8.402	547,452.3	356,421.3
	Auto-ETS	56.247	6.647	5.315	401,252.8	192,894.6
	Hyper-Tree-AR	58.352	7.183	5.880	453,636.0	247,230.1
	Hyper-Tree-ES	60.297	7.510	6.347	421,150.6	213,325.9
	LightGBM	55.554	6.815	5.453	423,425.8	222,984.1
	LightGBM-AR	60.767	8.723	7.534	536,273.0	336,581.1
	LightGBM-STL	47.886	9.197	7.368	467,240.7	301,457.0
Australian Retail Turnover	AR	9.079	9.078	9.118	30.666	24.442
	AR-X	8.316	8.305	8.368	27.563	21.719
	Auto-Arima	7.376	7.419	7.322	18.613	16.260
	Auto-Arima-X	7.537	7.543	7.553	21.365	18.289
	Auto-ETS	6.079	6.093	6.096	17.104	13.997
	Hyper-Tree-AR	6.958	6.771	6.949	19.645	16.770
	Hyper-Tree-ES	6.679	6.740	6.697	19.767	16.551
	LightGBM	9.097	8.871	8.950	20.045	17.005
	LightGBM-AR	9.980	9.422	9.983	27.076	22.521
	LightGBM-STL	11.038	11.205	11.210	27.768	23.909
Tourism	AR	25.048	21.846	20.280	2,976.6	2,289.4
	AR-X	24.930	21.634	19.909	2,924.7	2,239.8
	Auto-Arima	21.515	20.436	18.862	2,728.3	2,199.9
	Auto-Arima-X	21.088	20.067	18.719	2,773.1	2,207.3
	Auto-ETS	20.882	19.326	18.530	2,735.0	2,163.9
	Hyper-Tree-AR	29.850	20.881	21.337	3,474.0	2,815.9
	Hyper-Tree-ES	21.275	18.835	17.866	2,354.2	1,808.4
	LightGBM	32.575	26.389	23.399	4,475.4	3,943.5
	LightGBM-AR	32.443	24.796	24.999	4,743.7	3,474.4
	LightGBM-STL	28.125	26.093	24.953	3,967.6	3,230.1

Forecast-error metrics, lower is better. The best metrics are in bold. Reported are the mean values across all series. Mean Absolute Percentage Error (MAPE); Symmetric Mean Absolute Percentage Error (sMAPE); Weighted Absolute Percentage Error (WAPE); Root Mean Squared Error (RMSE); Mean Absolute Error (MAE).

The results presented in Table 2 indicate that the Hyper-Tree models demonstrate robust performance, often competing with or outperforming established forecasting methods. For the Australian Electricity Demand dataset, the Hyper-Tree-AR performs well and outperforms its classical autoregressive counterpart for some error metrics. In the case of the Australian Retail Turnover dataset, characterized by a pronounced trend and seasonality, both Hyper-Tree models demonstrate strong performance. The Hyper-Tree-ES model ranks second only to Auto-ETS, with the Hyper-Tree-AR following closely. This suggests that the Hyper-Tree approach effectively combines the strengths of tree-based models with the temporal dynamics captured by the inductive bias of the target models. Notably, compared to its classical counterparts AR and AR-X, the Hyper-Tree-AR outperforms both for the Australian Electricity Demand and Australian Retail Turnover datasets. This underscores the versatility and effectiveness of the Hyper-Tree approach in capturing complex temporal patterns. For the Tourism dataset, the Hyper-Tree-ES model shows a strong performance, despite using fixed parameters. Notably, the Hyper-Tree-ES outperforms all other models,

including its classical counterpart Auto-ETS, across all error metrics except MAPE. This demonstrates the robustness of exponential smoothing models, producing highly accurate forecasts even with manually set parameters.

4.3 Global Time Series Models

In previous sections, we evaluated Hyper-Trees in a local forecasting setting, training models for each time series individually without leveraging cross-series and feature information other than time-derived. We now turn our attention to global forecasting (Januschowski et al., 2020). Our Hyper-Tree approach is specifically designed for complex, operational forecasting tasks involving multiple time series. This global approach allows the model to capture shared patterns and dynamics across multiple time series, potentially improving forecasting accuracy and robustness, especially for datasets with common underlying factors. Operational forecasting typically involves datasets with missing values and high-dimensional feature sets that go beyond basic time series information, including, e.g., sales campaigns, calendar events, and categorical meta-features. In such environments, tree-based models typically excel, and Hyper-Trees are expected to perform well. To provide a more realistic testing ground for our approach, we add the Rossmann and M5 datasets that closely resemble real-world corporate datasets, in addition to the datasets used in the local forecasting evaluation. Additionally, we also add the commonly used M3 Monthly dataset. For our global forecasting evaluation, we exclude local forecasting models from the comparison, including LightGBM-STL. This decision stems from their inherent limitations in handling complex, multi-series forecasting tasks. Unlike global models, local models cannot leverage cross-series information, as they are typically trained on individual time series in isolation. This limitation in learning from multiple series simultaneously hinders their ability to capture broader patterns across the entire dataset, potentially reducing their generalization capabilities (Montero-Manso and Hyndman, 2021). Furthermore, local models struggle to effectively incorporate categorical meta-features, which are crucial for borrowing strength across similar series.

Besides comparing our approach to conventional tree-based and deep learning models, we also include a foundational time series model in our evaluation. This inclusion reflects the recent trend in time series analysis and forecasting towards large-scale, pre-trained models. Among others, the most prominent include Chronos (Ansari et al., 2024), Moirai (Woo et al., 2024), Moment (Goswami et al., 2024), TimesFM (Das et al., 2024), Tiny Time Mixers (Ekambaram et al., 2024) and Lag-Llama (Rasul et al., 2024). Trained on extensive and diverse time series datasets, these models promise enhanced accuracy and generalization capabilities in forecasting tasks. While their performance in forecasting has been recognized, the utility of pre-trained models extends beyond mere forecasting. A key advantage of foundational models lies in their capacity to generate rich time series embeddings. Unlike traditional feature extraction methods such as ts-features (Hyndman et al., 2024) or ts-fresh (Christ et al., 2018), these embeddings potentially capture more nuanced and complex temporal relationships. Researchers and practitioners can leverage these representations as input features for other models, potentially enhancing performance across various time series applications without the need for extensive feature engineering. For our analysis, we leverage the feature generation capabilities of foundational models, specifically utilizing Chronos (Ansari et al., 2024) to create time series features for all tree-based models.³ The features are derived by averaging the embeddings over all time steps, resulting in a fixed-length representation of 769 embeddings for each series. The embeddings are generated using the train data and remain fixed for the test set. This approach allows us to capture the overall characteristics of each series, aiming to enhance accuracy and generalization capabilities across diverse time series datasets of tree-based models.

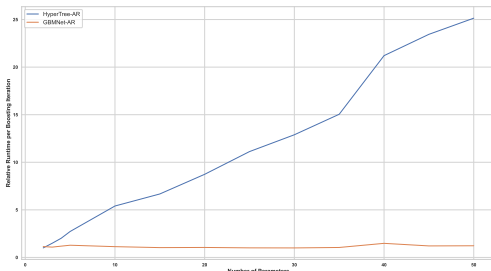
To ensure as fair a comparison as possible across models, we’ve made several decisions for our experimental setup. We disable the standard lag and time-feature generation in Deep-AR (Salinas et al., 2020) and TFT (Lim et al., 2021). Instead, we use the same lag specification and time-derived features across all models, with the exception of the time series embeddings which are unique to tree-models. This standardization allows for a more direct comparison of model performance. We estimate the 50% quantile using TFT (Lim et al., 2021), while for Deep-AR (Salinas et al., 2020), we calculate the mean from 1,000 samples drawn from a forecasted Student-T distribution. In the case of Chronos (Ansari et al., 2024), we use the t5-base version with default parameters and draw 50 samples from the forecasted distribution. We evaluate the Hyper-Tree-ES model only for datasets exhibiting stable seasonality across series, which excludes the M3, M5 and Rossmann datasets. Additionally, we remove series from the Tourism dataset that lacked consistent monthly seasonality. This selective approach is necessary because the global Hyper-Tree-ES expects stable seasonal patterns across all series. Including non-seasonal or irregularly seasonal series compromises parameter estimation and overall model performance. Further, the vectorized Hyper-Tree-ES estimation requires uniform series lengths, with the data structured in a tensor of shape (number of series, context-length, number of channels). This format allows for efficient vectorized estimation across multiple time series but necessitates that all series have the same length within a given dataset. For datasets with varying series lengths, we employ the following strategy: instead

³According to Ansari et al. (2024), the Chronos model was not pre-trained on any of the datasets used in our evaluation. All forecasts produced by Chronos (Ansari et al., 2024) are zero-shot, with no fine-tuning on any of the datasets used in our evaluation.

of using zeros or constants, we back-append a segment from the series itself to reach the length of the longest series. This method preserves the series’ characteristics and seasonality preventing distortion of seasonality initialization and estimation that would occur with constant or zero-padding. We also include a binary flag to identify padded observations as an additional feature.

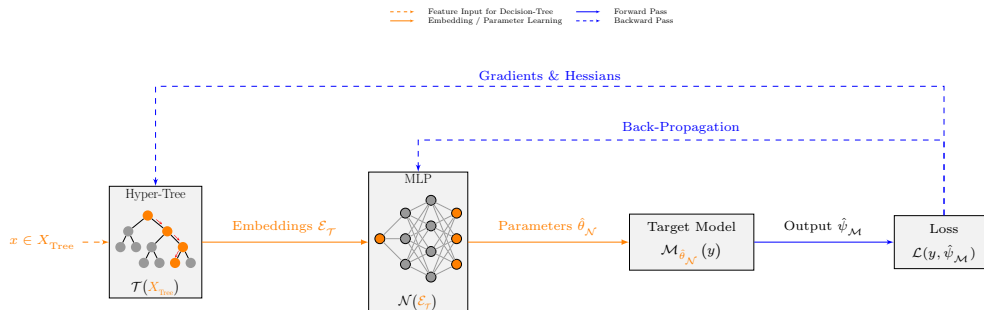
Before discussing the results in Table 3, it’s crucial to address the scaling issue inherent to GBDTs. Traditionally, GBDTs employ a one-vs-all strategy, growing a separate tree for each parameter. While effective for a small number of parameters, this approach scales poorly as the number of parameters increases (Iosipoi and Vakhrushev, 2022). The scaling issue mostly affects the Hyper-Tree-AR, particularly when a high number of lags is used, such as for weekly or daily datasets. The scaling issue is illustrated by the blue line in Figure 7, where we plot the relative runtime per boosting iteration using the Rossmann dataset for the Hyper-Tree-AR model estimated with the one-vs-all strategy.

Figure 7: Scaling Performance Comparison.



To overcome this limitation and to maintain the scalability of our framework, we propose a novel architecture that combines GBDTs with neural networks. We term this model GBM-Net, represented by the orange line in Figure 7. Clearly, it maintains a nearly constant runtime regardless of the number of parameters. Our hybrid approach utilizes GBDTs to generate low-dimensional embeddings, which are then transformed by a random projection matrix before serving as input to a shallow neural network, typically an MLP. The GBM-Net architecture illustrated in Figure 8 resembles an encoder-decoder framework, where the GBDT part acts as an encoder for the input features, and the MLP functions as a decoder, mapping the embeddings to the target model parameters.

Figure 8: GBM-Net Architecture.



The random projection matrix, incorporated as an initial layer with fixed parameters, expands the tree embeddings into a higher-dimensional space. This expansion diversifies the representations and increases the input dimensions for the subsequent neural network, enhancing its learning capacity. For all experiments, we use a one-dimensional tree-embedding to keep the runtimes low. While higher-dimensional embeddings can be used as well, this comes at the cost of increased runtime. We experimented with higher embedding dimensions but found that a one-dimensional embedding combined with the random projection matrix offers a good trade-off between accuracy and runtime. Importantly, instead of using also the original features, only the tree-embeddings are used as input to the MLP, leveraging the GBDT’s ability to effectively encode both categorical and numeric features. Our choice of an MLP is primarily motivated by its lightweight architecture, complemented by recent findings in the time series literature, suggesting that MLP-type models are competitive with more complex architectures (Zeng et al., 2023; Chen et al., 2023; Ekambaram et al., 2023). Both the GBDTs and the MLP are trained jointly, rather than in a two-step procedure. This joint learning leads to improved performance by leveraging the interplay between feature learning and parameter mapping. Our hybrid approach allows us to maintain the strengths of GBDTs while overcoming their scalability limitations when estimating a large number of target parameters. For all of our experiments, we employ a shallow MLP structure following the sequence

{Tree Embeddings \rightarrow Random Projection \rightarrow Hidden-Layer \rightarrow ReLU \rightarrow Output-Layer \rightarrow Dropout}. We maintain a fixed hidden dimension, dropout-rate, and learning rate for the MLPs across all datasets. The dimension of the random projection matrix is set to match the output dimension of the MLP, which corresponds to the number of target model parameters. For the GBM-Net model, we experimented with different batch training approaches, including batch training for both GBDTs and MLP, and batch training for MLP only while using all data for GBDTs. We found that using no batch training yields the best results. This might be attributed to the GBDT’s ability to capture global patterns and relationships more effectively when using all data, potentially leading to more informative tree embeddings. We now turn to the discussion of the results presented in Table 3.

Table 3: Global Model Results.

Dataset	Model	MAPE	sMAPE	WAPE	RMSE	MAE	Runtime (Minutes)
Australian Electricity Demand	Chronos	55.485	6.649	5.261	389,282.6	191,161.8	0.021
	Deep-AR	55.889	6.672	5.249	436,737.6	217,696.8	1.678
	GBM-Net-AR	56.639	6.572	5.226	422,328.0	211,209.8	0.011
	Hyper-Tree-AR	58.291	7.159	5.854	453,321.7	246,868.0	0.040
	Hyper-Tree-ES	60.763	8.104	6.987	447,684.3	239,975.6	3.629
	LightGBM	62.915	9.993	8.992	545,426.0	358,366.6	0.002
	LightGBM-AR	60.284	8.308	7.091	480,051.0	285,219.4	0.004
	TFT	58.767	8.405	7.071	461,571.8	274,424.9	2.254
Australian Retail Turnover	Chronos	7.117	6.914	7.026	18.166	15.832	1.190
	Deep-AR	7.995	7.581	7.914	20.662	18.209	5.747
	GBM-Net-AR	6.278	6.213	6.325	15.982	13.147	0.542
	Hyper-Tree-AR	6.842	6.621	6.827	19.618	16.729	4.465
	Hyper-Tree-ES	6.582	6.653	6.616	19.809	16.594	36.987
	LightGBM	14.524	12.584	14.235	22.374	19.451	0.184
	LightGBM-AR	7.891	7.618	7.838	21.439	18.176	0.172
	TFT	9.756	9.085	9.669	26.250	22.725	10.153
M3 Monthly	Chronos	16.668	13.874	13.724	751.987	618.140	3.911
	Deep-AR	22.756	15.359	15.661	859.278	715.211	3.021
	Hyper-Tree-AR	19.926	14.535	14.651	807.201	669.392	2.398
	Hyper-Tree-ES	–	–	–	–	–	–
	GBM-Net-AR	20.121	14.811	14.821	823.370	685.608	0.314
	LightGBM	34.068	26.178	27.897	1,350.5	1,235.8	0.277
	LightGBM-AR	22.555	14.555	14.984	791.244	660.090	0.208
	TFT	19.752	14.657	14.551	796.385	653.173	3.722
M5	Chronos	13.997	13.326	13.274	81.722	63.557	0.843
	Deep-AR	14.874	13.592	13.718	80.724	64.280	2.984
	GBM-Net-AR	14.909	13.301	13.488	76.717	61.003	0.428
	Hyper-Tree-AR	17.745	15.002	15.724	93.646	76.753	3.163
	Hyper-Tree-ES	–	–	–	–	–	–
	LightGBM	17.873	18.894	18.104	112.324	94.750	0.235
	LightGBM-AR	14.862	13.550	13.729	88.838	71.956	0.223
	TFT	14.600	13.736	13.758	85.118	68.688	4.382
Rossmann Store Sales	Chronos	12.799	12.260	12.284	1,140.4	857.111	18.464
	Deep-AR	10.893	10.149	10.475	945.087	725.977	7.124
	GBM-Net-AR	9.329	9.363	9.268	842.550	648.724	3.897
	Hyper-Tree-AR	8.469	8.571	8.494	773.052	596.919	48.629
	Hyper-Tree-ES	–	–	–	–	–	–
	LightGBM	13.643	13.264	13.405	1,147.5	914.963	4.470
	LightGBM-AR	10.799	10.285	10.445	916.604	717.592	3.829
	TFT	10.518	9.835	10.108	916.373	701.574	10.115
Tourism	Chronos	39.362	38.494	36.550	4,698.9	3,796.7	1.639
	Deep-AR	34.448	26.916	29.189	4,373.9	3,645.4	6.931
	GBM-Net-AR	33.032	27.775	27.760	3,799.2	3,268.0	0.429
	Hyper-Tree-AR	28.038	25.144	24.341	3,769.2	3,248.6	4.560
	Hyper-Tree-ES	32.279	30.726	25.420	4,116.0	3,301.1	35.712
	LightGBM	50.795	69.555	51.532	10,333.0	9,746.9	0.225
	LightGBM-AR	44.226	31.920	32.436	4,408.6	3,634.7	0.188
	TFT	40.267	29.570	33.175	5,051.3	4,146.8	9.307

Forecast-error metrics and runtimes, lower is better. The best metrics are in bold. Reported are the mean-errors across all series and total runtimes in minutes. Mean Absolute Percentage Error (MAPE); Symmetric Mean Absolute Percentage Error (sMAPE); Weighted Absolute Percentage Error (WAPE); Root Mean Squared Error (RMSE); Mean Absolute Error (MAE). Entries with “–” indicate that the model was not estimated.

The Hyper-Tree and GBM-Net models demonstrate competitive performance across various datasets. The Hyper-Tree-AR model excels for both the Tourism and the Rossmann Store Sales dataset, outperforming all other models across all metrics, albeit at the cost of higher runtimes. For the Rossmann Store Sales dataset with an AR(21) specification, the runtime-efficient GBM-Net-AR offers a favorable trade-off, with only slightly lower accuracy but much faster runtime. Our Hyper-Tree-ES performs well on datasets with pronounced and stable seasonality, such as Australian Retail Turnover and Tourism, ranking a close second to Hyper-Tree-AR for the latter. However, due to its recursive nature, Hyper-Tree-ES generally exhibits the highest runtime among all models, which may limit its practical applicability in time-sensitive scenarios. The GBM-Net-AR model consistently achieves high accuracy while maintaining computational efficiency. It outperforms other models in terms of WAPE and sMAPE, while ranking second in MAPE for the Australian Electricity Demand dataset. For the Australian Retail Turnover dataset, it achieves the highest accuracy across all error metrics, while for the M5 dataset, it closely follows Chronos (Ansari et al., 2024) in accuracy. Notably, GBM-Net-AR achieves runtimes comparable to its classical LightGBM counterparts while typically delivering higher accuracy, making it a favorable choice when balancing performance and computational cost. For the M3 Monthly dataset, Chronos (Ansari et al., 2024) demonstrates superior performance across all error metrics, albeit with a relatively high runtime. Generally, the results in Table 3 suggest that our Hyper-Tree architectures are effective across diverse datasets, often matching or exceeding the performance of established forecasting methods. As expected, our architecture performs particularly well on complex, operational time series, such as Rossmann Store Sales and M5, with features that go beyond basic time series information. For the Rossmann Store Sales dataset, both of our models achieve the highest accuracy, with the GBM-Net ranking second behind the Hyper-Tree-AR model. For some datasets, the GBM-Net-AR model outperforms the Hyper-Tree-AR model, highlighting the advantages of the hybrid approach.

Given the competitive accuracy of our Hyper-Trees across multiple datasets, it remains open to investigate the underlying reasons for this. In the following, we postulate several factors that contribute to their performance. One key aspect is that Hyper-Trees operate in parameter space rather than directly in the forecast space, offering advantages in robustness and generalizability. In the forecast space, each dimension represents a future time point with values potentially ranging from negative to positive infinity. This unconstrained space can complicate the modeling of complex temporal dependencies and hinder generalization across diverse series. In contrast, the parameter space provides a more constrained and structured setting. Parameters of time series models, such as autoregressive coefficients, are often bounded by stationarity conditions and possess clear interpretations within the model framework. The structural constraints inherent in the parameter space supply a strong inductive bias, steering the learning process toward more stable solutions. For example, in an AR(p) model, parameters signify the influence of past observations, typically diminishing with higher-order lags. This intrinsic structure aids in capturing meaningful temporal patterns that can generalize across different series, even when they exhibit heterogeneous behaviors. Operating in the parameter space also enhances interpretability and facilitates the incorporation of domain knowledge. Parameters with clear practical or theoretical meanings allow for easier validation and alignment with expert insights. As such, known constraints such as domain-specific knowledge can be readily encoded into the parameter space, improving the model’s ability to produce consistent and plausible forecasts. Related to operating in the parameter space is the advantage of our Hyper-Tree approach to generate dynamic, non-stationary parameters. By modeling and forecasting parameters as a function of features, Hyper-Trees can adjust parameters dynamically, responding to evolving patterns in the data. This flexibility enables Hyper-Trees to capture changing patterns more effectively than models with fixed parameters. The inductive bias induced by the target model plays a crucial role as well. By learning to generate parameters for specific time series models, the Hyper-Trees inherit the underlying assumptions and structures of these models. This allows them to capture meaningful temporal patterns that can generalize across different series. Another key strength of the Hyper-Tree approach lies in its ability to learn a global mapping from input features to model parameters, which are then applied locally to each series. This effectively balances global learning with local adaptation, addressing the challenge of heterogeneity in global models. Unlike traditional decision tree models that forecast time series directly, Hyper-Trees can mitigate the distortions that can occur when heterogeneous series with different magnitudes and behaviors end up in the same terminal node. When forecasting directly, these differences can significantly impact forecast quality, especially in operational forecasting tasks where there’s often a lack of known or unknown features to properly separate diverse series. The Hyper-Tree’s approach mitigates this issue by generating parameters that adapt to local characteristics when applied to individual series. Even if similar parameter values are assigned to heterogeneous series, applying these parameters to each series results in distinct, series-specific forecasts. This localization effect enables Hyper-Trees to handle time series effectively within a heterogeneous dataset. The Hyper-Trees’ adaptivity allows for nuanced forecasts that respect each series’ unique properties while still leveraging patterns learned across the entire dataset. As a result, Hyper-Trees can produce more accurate and tailored forecasts for heterogeneous time series, overcoming the limitations often faced by traditional decision tree models in global forecasting scenarios.

4.3.1 Ablation Studies

In this section, we conduct a series of ablation studies. By systematically removing or modifying components, we aim to gain deeper insights into the contribution of each model element to overall accuracy for the Hyper-Tree-AR and GBM-Net-AR model. Our experiments use the operational Rossmann Store Sales dataset. Its scale in terms of available time series and its complexity mimic those encountered in practical business forecasting problems, providing a suitable environment for evaluating the sensitivity of our models to various components. For our ablation studies, we have chosen the following modifications:

- A1: Increase the dimension of tree-embeddings from 1 to 10.
- A2: Remove linear-tree option of [Shi et al. \(2019\)](#).
- A3: Increase hidden-dimension of the MLP from 128 to 256.
- A4: Remove random projection layer.
- A5: Reduce number of lags to from 21 to 14.
- A6: Exclude Chronos ([Ansari et al., 2024](#)) embeddings.
- A7: Exclude GBDTs as encoding layer and use MLP only.
- A8: Use GBM-Net to forecast directly, without learning parameters of a target model.

Each variant (A1 - A8) is derived from the Base model as reported in Table 3, with a specific modification applied to create each variation. This approach allows us to isolate and evaluate the impact of individual components. Table 4 shows the results.

Table 4: Rossmann Ablation Study Results.

Model	Ablation	MAPE	sMAPE	WAPE	RMSE	MAE
GBM-Net-AR	Base	9.329	9.363	9.268	842.550	648.724
	A1	9.039	9.071	9.141	852.538	638.087
	A2	9.643	9.626	9.543	867.644	668.017
	A3	9.654	9.792	9.621	871.243	674.822
	A4	10.225	10.063	9.953	892.814	696.827
	A5	10.084	10.208	10.011	900.097	701.802
	A6	11.511	11.350	10.972	978.613	766.371
	A7	16.885	15.906	15.826	1,374.9	1,113.3
	A8	15.765	16.417	15.866	1,389.0	1,154.4
Hyper-Tree-AR	Base	8.469	8.571	8.494	773.052	596.919
	A2	8.389	8.514	8.400	754.675	588.699
	A5	9.576	8.963	9.641	940.139	693.643
	A6	10.463	10.642	10.407	927.370	718.675

Forecast-error metrics, lower is better. The best metrics are in bold. Reported are the mean-errors across all series. Mean Absolute Percentage Error (MAPE); Symmetric Mean Absolute Percentage Error (sMAPE); Weighted Absolute Percentage Error (WAPE); Root Mean Squared Error (RMSE); Mean Absolute Error (MAE).

The ablation study results for the GBM-Net-AR model reveal interesting insights into the model’s components. Increasing the dimension of tree-embeddings (A1) leads to the only improvement. This suggests that higher-dimensional tree embeddings can capture more nuanced patterns in the data. However, this enhanced performance comes at the cost of an increase in runtime. Moving to A2, which removes the linear-tree option, we observe a slight performance degradation. Similarly, increasing the MLP hidden dimension (A3) shows a minor decline in accuracy. The impact becomes more pronounced with the removal of the random projection layer (A4), leading to a more pronounced drop in accuracy. This underscores the importance of diversifying the low dimensional tree embeddings to maintain high accuracy. Further, reducing the number of lags (A5) results in a decline in performance, suggesting that the original lag structure captured important temporal dependencies that are lost with fewer lags. Excluding the embeddings (A6) shows a substantial accuracy degradation compared to the Base model across all metrics. It is worth noting that the removal of the 769 embeddings significantly reduces the computational cost. Specifically, the average runtime per epoch decreases from 3.7 seconds for the Base model to only 0.6 seconds without the embeddings. This presents an interesting trade-off between accuracy and computational efficiency that practitioners may need to consider based on their specific requirements and resources. A significant drop in accuracy is observed for A7, where GBDTs are excluded as the encoding layer and an MLP is used only. This performance degradation underscores the crucial role of GBDTs in effectively processing

and encoding the input features into informative embeddings for the MLP. The results of A7 therefore highlight the synergistic effect of combining GBDTs with neural networks in our GBM-Net architecture. The most substantial drop in accuracy is observed for A8, with the "Hyper"-part being removed and the GBM-Net being used to forecast directly without learning the parameters of a target model. This significant degradation in accuracy suggests that learning the parameters of a target model is crucial for the GBM-Net's effectiveness. The hyper-model approach, operating in the parameter space rather than the forecast space, proves beneficial. It preserves crucial information lost in direct forecasting, as evidenced by the significant drop in accuracy. This underscores the importance of the two-stage approach in the Base model. Turning to the Hyper-Tree-AR model, Table 4 shows that while removing the linear-tree option negatively impacts the GBM-Net-AR model, it has a positive effect on the accuracy of the Hyper-Tree-AR. Apart from this, the Hyper-Tree-AR model shows similar sensitivities to lag reduction (A5) and the exclusion of embeddings (A6) as observed for the GBM-Net-AR model. Notably, the exclusion of the embeddings results in a substantial accuracy degradation, mirroring the effect seen for the GBM-Net-AR model. This consistency across models highlights the potential of using foundational models to generate informative embeddings that can serve as informative features, effectively capturing temporal dynamics for accurate global forecasting.

5 Conclusion and Future Research

With our Hyper-Tree framework, we have ventured into the uncharted territory of using tree-based models for learning and forecasting parameters that are used as input for target time series models. By designing GBDTs to learn the parameters of time series models, we have combined the strengths of boosted trees with the advantages of established time series models. This approach naturally induces a time series inductive bias to tree models and addresses the challenge of parameter non-stationarity. We also suggest a novel approach to resolve the inherent scaling issue of GBDTs, contributing to the growing literature on combining decision trees and neural networks within a unified framework. In this hybrid approach, the tree serves as an encoding layer, transforming features into informative representations, while the network functions as a decoder, mapping these embeddings to the target model parameters. As a first step, we explored the effectiveness of our framework across several forecasting scenarios and datasets. Our findings underscore the potential of tree-based models in learning parameters that are input to other models, bridging the gap between traditional forecasting tasks and tree-based modeling, thereby showcasing a novel approach that opens new ways of understanding and utilizing tree-based models beyond their conventional applications.

Looking forward, the horizon of future research in this domain is broad and inviting. While our study has laid the groundwork for tree-based hyper-models, there remain several compelling avenues for further investigation. Our current focus on training relatively simple target models opens up opportunities to explore the applicability of our approach to more complex architectures. Exploring state space formulations would offer a unified and flexible framework for modeling complex temporal dynamics. Also, extending the framework to include automated model and lag selection would enhance the adaptability of our Hyper-Tree models further. Additionally, improving the runtime efficiency of Hyper-Tree-ES would broaden its applicability to larger-scale problems, making it a more versatile tool for diverse time series forecasting scenarios. The cross-learning abilities of tree-based models present another interesting direction for future research. Leveraging these capabilities to enable domain adaptation or few-shot learning could significantly enhance the versatility of Hyper-Trees in real-world applications. A probabilistic extension of our approach also merits consideration. Incorporating uncertainty quantification into the Hyper-Tree framework would offer a more comprehensive understanding of the underlying time series dynamics. In addition to these extensions, the combination of trees and networks opens up new possibilities to leverage the strengths of both tree-based models and neural network architectures, leading to even more flexible time series modeling capabilities. This future direction not only extends our current work but also further bridges the gap between tree-based and deep learning approaches.

Implementation

The code will be made available on the official repository <https://github.com/StatMixedML/Hyper-Trees> upon the final publication of this paper.

References

- Alexandrov, A., Benidis, K., Bohlke-Schneider, M., Flunkert, V., Gasthaus, J., Januschowski, T., Maddix, D. C., Rangapuram, S., Salinas, D., Schulz, J., Stella, L., Türkmen, A. C., and Wang, Y. (2020). Gluonts: Probabilistic and neural time series modeling in python. *Journal of Machine Learning Research*, 21(116):1–6.
- Ansari, A. F., Stella, L., Turkmen, C., Zhang, X., Mercado, P., Shen, H., Shchur, O., Rangapuram, S. S., Arango, S. P., Kapoor, S., Zschiegner, J., Maddix, D. C., Wang, H., Mahoney, M. W., Torkkola, K., Wilson, A. G., Bohlke-Schneider, M., and Wang, Y. (2024). Chronos: Learning the language of time series. *ArXiv*.
- Athanasopoulos, G., Hyndman, R. J., Song, H., and Wu, D. C. (2011). The tourism forecasting competition. *International Journal of Forecasting*, 27(3):822–844.
- Badirli, S., Liu, X., Xing, Z., Bhowmik, A., and Keerthi, S. S. (2020). Gradient boosting neural networks: Grownet. *ArXiv*, abs/2002.07971.
- Bansal, M. A., Sharma, R., and Kathuria, M. (2022). A systematic review on data scarcity problem in deep learning: Solution and applications. *ACM Comput. Surv.*, 54(10s).
- Bollerslev, T. (1986). Generalized autoregressive conditional heteroskedasticity. *Journal of Econometrics*, 31(3):307–327.
- Box, G. E. P., Jenkins, G. M., Reinsel, G. C., and Ljung, G. M. (2015). *Time Series Analysis: Forecasting and Control*. Wiley Series in Probability and Statistics. Wiley, 5th edition edition.
- Casale, P., Pujol, O., and Radeva, P. (2011). Embedding random projections in regularized gradient boosting machines. In Okun, O., Valentini, G., and Re, M., editors, *Ensembles in Machine Learning Applications*, pages 201–216. Springer Berlin Heidelberg, Berlin, Heidelberg.
- Chen, S.-A., Li, C.-L., Arik, S. O., Yoder, N. C., and Pfister, T. (2023). Tsmixer: An all-mlp architecture for time series forecasting. *Transactions on Machine Learning Research*.
- Chen, T. and Guestrin, C. (2016). Xgboost: A scalable tree boosting system. In *Proceedings of the 22nd ACM SIGKDD International Conference on Knowledge Discovery and Data Mining*, KDD '16, pages 785–794.
- Cho, K., van Merriënboer, B., Gulcehre, C., Bahdanau, D., Bougares, F., Schwenk, H., and Bengio, Y. (2014). Learning phrase representations using rnn encoder–decoder for statistical machine translation. In Moschitti, A., Pang, B., and Daelemans, W., editors, *Proceedings of the 2014 Conference on Empirical Methods in Natural Language Processing (EMNLP)*, pages 1724–1734, Doha, Qatar. Association for Computational Linguistics.
- Christ, M., Braun, N., Neuffer, J., and Kempa-Liehr, A. W. (2018). Time series feature extraction on basis of scalable hypothesis tests (tsfresh – a python package). *Neurocomputing*, 307:72–77.
- Cleveland, R. B., Cleveland, W. S., McRae, J. E., and Terpenning, I. J. (1990). Stl: A seasonal-trend decomposition procedure based on loess. *Journal of Official Statistics*, 6(1):3–33.
- Das, A., Kong, W., Sen, R., and Zhou, Y. (2024). A decoder-only foundation model for time-series forecasting. *ArXiv*.
- de Vito, L. (2017). Linxgboost: Extension of xgboost to generalized local linear models. *arXiv Pre-Print*, pages 1–12.
- Duan, T., Anand, A., Ding, D. Y., Thai, K. K., Basu, S., Ng, A. Y., and Schuler, A. (2020). Ngboost: Natural gradient boosting for probabilistic prediction. In *Proceedings of the 37th International Conference on Machine Learning, ICML 2020, 13-18 July 2020, Virtual Event*, volume 119 of *Proceedings of Machine Learning Research*, pages 2690–2700. PMLR.
- Duan, W., He, X., Zhou, L., Thiele, L., and Rao, H. (2022). Combating distribution shift for accurate time series forecasting via hypernetworks. In *2022 IEEE 28th International Conference on Parallel and Distributed Systems (ICPADS)*, pages 900–907, Los Alamitos, CA, USA. IEEE Computer Society.
- Ekambaram, V., Jati, A., Dayama, P., Mukherjee, S., Nguyen, N. H., Gifford, W. M., Reddy, C., and Kalagnanam, J. (2024). Tiny time mixers (ttms): Fast pre-trained models for enhanced zero/few-shot forecasting of multivariate time series. *ArXiv*.
- Ekambaram, V., Jati, A., Nguyen, N., Sinthong, P., and Kalagnanam, J. (2023). Tsmixer: Lightweight mlp-mixer model for multivariate time series forecasting. In *Proceedings of the 29th ACM SIGKDD Conference on Knowledge Discovery and Data Mining*, KDD '23, pages 459–469, New York, NY, USA. Association for Computing Machinery.
- Emami, S. and Martínez-Muñoz, G. (2022). Multioutput regression neural network training via gradient boosting. *ESANN 2022 proceedings*.
- Engle, R. F. (1982). Autoregressive conditional heteroskedasticity with estimates of the variance of united kingdom inflation. *Econometrica*, 50(4):987–1007.

- Fons, E., Sztrajman, A., El-Laham, Y., Iosifidis, A., and Vyetrenko, S. (2022). Hypertime: Implicit neural representations for time series. In *NeurIPS 2022 Workshop on Synthetic Data for Empowering ML Research*.
- Friedman, J. H. (2001). Greedy function approximation: A gradient boosting machine. *The Annals of Statistics*, 29(5):1189–1232.
- Garza, F., Mergenthaler Canseco, M., Challú, C., and Olivares, K. G. (2022). Statsforecast: Lightning fast forecasting with statistical and econometric models. *PyCon Salt Lake City, Utah, US 2022*, <https://github.com/Nixtla/statsforecast>.
- Godaheva, R., Bergmeir, C., Webb, G. I., Hyndman, R. J., and Montero-Manso, P. (2021). Monash time series forecasting archive. In *Neural Information Processing Systems Track on Datasets and Benchmarks*.
- Godaheva, R., Webb, G. I., Schmidt, D., and Bergmeir, C. (2023). Setar-tree: a novel and accurate tree algorithm for global time series forecasting. *Machine Learning*, 112(7):2555–2591.
- Goswami, M., Szafer, K., Choudhry, A., Cai, Y., Li, S., and Dubrawski, A. (2024). Moment: A family of open time-series foundation models. *ArXiv*.
- Ha, D., Dai, A. M., and Le, Q. V. (2017). Hypernetworks. In *International Conference on Learning Representations*.
- Hasson, H., Wang, B., Januschowski, T., and Gasthaus, J. (2021). Probabilistic forecasting: A level-set approach. In Beygelzimer, A., Dauphin, Y., Liang, P., and Wortman Vaughan, J., editors, *Advances in Neural Information Processing Systems*.
- Hochreiter, S. and Schmidhuber, J. (1997). Long short-term memory. *Neural Comput*, 9(8):1735–1780.
- Holt, C. C. (1957). Forecasting seasonals and trends by exponentially weighted moving averages. (*ONR Memorandum No. 52*). *Carnegie Institute of Technology, Pittsburgh USA. Reprinted in the International Journal of Forecasting 2004*, 20(1):5–10.
- Horrell, M. T. (2024). Gradient boosting modules for pytorch.
- Hyndman, R., Kang, Y., Montero-Manso, P., O’Hara-Wild, M., Talagala, T., Wang, E., and Yang, Y. (2024). tsfeatures: Time series feature extraction.
- Hyndman, R. J. and Athanasopoulos, G. (2021). *Forecasting: Principles and Practice*. OTexts, Australia, 3rd edition.
- Iosipoi, L. and Vakhrushev, A. (2022). Sketchboost: fast gradient boosted decision tree for multioutput problems. In *Proceedings of the 36th International Conference on Neural Information Processing Systems, NIPS ’22*, Red Hook, NY, USA. Curran Associates Inc.
- Januschowski, T., Gasthaus, J., Wang, Y., Salinas, D., Flunkert, V., Bohlke-Schneider, M., and Callot, L. (2020). Criteria for classifying forecasting methods. *International Journal of Forecasting*, 36(1):167–177.
- Januschowski, T. and Kolassa, S. (2019). A classification of business forecasting problems. *Foresight: The International Journal of Applied Forecasting*, 1(52):36–43.
- Januschowski, T., Wang, Y., Torkkola, K., Erkkilä, T., Hasson, H., and Gasthaus, J. (2022). Forecasting with trees. *International Journal of Forecasting*, 38(4):1473–1481.
- Johansson, U., Löfström, T., and Boström, H. (2023). Conformal predictive distribution trees. *Annals of Mathematics and Artificial Intelligence*.
- Karingula, S. R., Ramanan, N., Tahmasbi, R., Amjadi, M., Jung, D., Si, R., Thimmisetty, C., Polania, L. F., Sayer, M., Taylor, J., and Coelho, C. N. (2022). Boosted embeddings for time-series forecasting. In Nicosia, G., Ojha, V., La Malfa, E., La Malfa, G., Jansen, G., Pardalos, P. M., Giuffrida, G., and Umeton, R., editors, *Machine Learning, Optimization, and Data Science*, pages 1–14, Cham. Springer International Publishing.
- Ke, G., Meng, Q., Finley, T., Wang, T., Chen, W., Ma, W., Ye, Q., and Liu, T.-Y. (2017). Lightgbm: A highly efficient gradient boosting decision tree. In *Proceedings of the 31st International Conference on Neural Information Processing Systems, NIPS’17*, pages 3149–3157.
- Király, F., Löning, M., Bagnall, T., Middlehurst, M., Ganesh, S., Walter, M., Oastler, G., Lines, J., Ray, A., Kaz, V., Mentel, L., Heidrich, B., Mishra, S., holder, C., Bartling, D., Tsaprounis, L., Kuhns, R. N., Gilbert, C., Baichoo, M., Akmal, H., Guzal, Owoseni, T., Rockenschaub, P., eenticott shell, Alavi, S., jesellier, Manani, K., Schäfer, P., and Khrapov, S. (2024). sktime/sktime: v0.29.0.
- Knauer, F. and Cukierski, W. (2015). Rossmann store sales.
- Kontschieder, P., Fiterau, M., Criminisi, A., and Bulò, S. R. (2016). Deep neural decision forests. In *Proceedings of the Twenty-Fifth International Joint Conference on Artificial Intelligence, IJCAI’16*, pages 4190–4194. AAAI Press.
- Lee, J., Kim, C., Lee, G., Lim, H., Choi, J., Lee, K., Lee, D., Hong, S., and Park, N. (2023). Hypernetwork approximating future parameters for time series forecasting under temporal drifts. In *Advances in Neural Information Processing Systems Workshop on Distribution Shifts (NeurIPS DistShift)*, NIPS’2023, pages 1–17.

- Li, H., Song, J., Xue, M., Zhang, H., Ye, J., Cheng, L., and Song, M. (2023). A survey of neural trees. *ACM Computing Survey*, 1(1).
- Lim, B., Arik, S. Ö., Loeff, N., and Pfister, T. (2021). Temporal fusion transformers for interpretable multi-horizon time series forecasting. *International Journal of Forecasting*, 37(4):1748–1764.
- Löning, M., Bagnall, A., Ganesh, S., Kazakov, V., Lines, J., and Király, F. J. (2019). sktime: A unified interface for machine learning with time series. *Workshop on Systems for ML at NeurIPS 2019*.
- Lundberg, S. M., Erion, G., Chen, H., DeGrave, A., Prutkin, J. M., Nair, B., Katz, R., Himmelfarb, J., Bansal, N., and Lee, S.-I. (2020). From local explanations to global understanding with explainable ai for trees. *Nature Machine Intelligence*, 2(1):2522–5839.
- Lundberg, S. M. and Lee, S.-I. (2017). A unified approach to interpreting model predictions. In I. Guyon, U. V. Luxburg, S. Bengio, H. Wallach, R. Fergus, S. Vishwanathan, and R. Garnett, editors, *Advances in Neural Information Processing Systems 30*, pages 4765–4774. Curran Associates, Inc.
- Makridakis, S. and Hibon, M. (2000). The m3-competition: results, conclusions and implications. *International Journal of Forecasting*, 16(4):451–476.
- Makridakis, S., Spiliotis, E., and Assimakopoulos, V. (2022a). The m5 competition: Background, organization, and implementation. *International Journal of Forecasting*, 38(4):1325–1336.
- Makridakis, S., Spiliotis, E., Assimakopoulos, V., Chen, Z., Gaba, A., Tsetlin, I., and Winkler, R. L. (2022b). The m5 uncertainty competition: Results, findings and conclusions. *International Journal of Forecasting*, 38(4):1365–1385.
- März, A. (2019). Xgboostlss - an extension of xgboost to probabilistic forecasting. *arXiv Pre-Print*, pages 1–23.
- März, A. (2022). Multi-target xgboostlss regression. *arXiv Pre-Print*, pages 1–11.
- März, A. and Kneib, T. (2022). Distributional gradient boosting machines. *arXiv Pre-Print*, pages 1–15.
- Medeiros, M. C. and Veiga, A. (2000). A hybrid linear-neural model for time series forecasting. *IEEE Transactions on Neural Networks*, 11(6):1402–1412.
- Montero-Manso, P. and Hyndman, R. J. (2021). Principles and algorithms for forecasting groups of time series: Locality and globality. *International Journal of Forecasting*, 37(4):1632–1653.
- Nasios, I. and Vogklis, K. (2022). Blending gradient boosted trees and neural networks for point and probabilistic forecasting of hierarchical time series. *International Journal of Forecasting*, 38(4):1448–1459.
- O’Hara-Wild, M., Hyndman, R., Wang, E., and Godahewa, R. (2022). tsibbledata: Diverse datasets for ‘tsibble’.
- Paszke, A., Gross, S., Massa, F., Lerer, A., Bradbury, J., Chanan, G., Killeen, T., Lin, Z., Gimelshein, N., Antiga, L., Desmaison, A., Köpf, A., Yang, E., DeVito, Z., Raison, M., Tejani, A., Chilamkurthy, S., Steiner, B., Fang, L., Bai, J., and Chintala, S. (2019). Pytorch: An imperative style, high-performance deep learning library. In *Proceedings of the 33rd International Conference on Neural Information Processing Systems*, volume 721. Curran Associates Inc.
- Popov, S., Morozov, S., and Babenko, A. (2020). Neural oblivious decision ensembles for deep learning on tabular data. *8th International Conference on Learning Representations*.
- Prokhorenkova, L., Gusev, G., Vorobev, A., Dorogush, A. V., and Gulin, A. (2018). Catboost: unbiased boosting with categorical features. In S. Bengio, H. Wallach, H. Larochelle, K. Grauman, N. Cesa-Bianchi, and R. Garnett, editors, *Advances in Neural Information Processing Systems*, volume 31. Curran Associates, Inc.
- Rangapuram, S. S., Seeger, M. W., Gasthaus, J., Stella, L., Wang, Y., and Januschowski, T. (2018). Deep state space models for time series forecasting. In S. Bengio, H. Wallach, H. Larochelle, K. Grauman, N. Cesa-Bianchi, and R. Garnett, editors, *Advances in Neural Information Processing Systems*, volume 31. Curran Associates, Inc.
- Rasul, K., Ashok, A., Williams, A. R., Ghonia, H., Bhagwatkar, R., Khorasani, A., Bayazi, M. J. D., Adamopoulos, G., Riachi, R., Hassen, N., Biloš, M., Garg, S., Schneider, A., Chapados, N., Drouin, A., Zantedeschi, V., Nevmyvaka, Y., and Rish, I. (2024). Lag-llama: Towards foundation models for probabilistic time series forecasting. *ArXiv*.
- Romano, Y., Patterson, E., and Candès, E. J. (2019). Conformalized quantile regression. In *Proceedings of the 33rd International Conference on Neural Information Processing Systems*. Curran Associates Inc, Red Hook, NY, USA.
- Salinas, D., Flunkert, V., Gasthaus, J., and Januschowski, T. (2020). Deepar: Probabilistic forecasting with autoregressive recurrent networks. *International Journal of Forecasting*, 36(3):1181–1191.
- Seabold, S. and Perktold, J. (2010). statsmodels: Econometric and statistical modeling with python. In *9th Python in Science Conference*.
- Shi, Y., Li, J., and Li, Z. (2019). Gradient boosting with piece-wise linear regression trees. In *Proceedings of the 28th International Joint Conference on Artificial Intelligence, IJCAI’19*, pages 3432–3438. AAAI Press.

- Sigrist, F. (2021). Gradient and newton boosting for classification and regression. *Expert Systems with Applications*, 167:114080.
- Sprangers, O., Schelter, S., and de Rijke, M. (2021). Probabilistic gradient boosting machines for large-scale probabilistic regression. In *Proceedings of the 27th ACM SIGKDD Conference on Knowledge Discovery & Data Mining*, KDD '21, pages 1510–1520.
- Sprangers, O., Schelter, S., and de Rijke, M. (2023). Parameter-efficient deep probabilistic forecasting. *International Journal of Forecasting*, 39(1):332–345.
- Vogelsgesang, A., Haubenschild, M., Finis, J., Kemper, A., Leis, V., Muehlbauer, T., Neumann, T., and Then, M. (2018). Get real: How benchmarks fail to represent the real world. In *Proceedings of the Workshop on Testing Database Systems*, DBTest'18, New York, NY, USA. Association for Computing Machinery.
- Vovk, V., Gammerman, A., and Shafer, G. (2022). *Algorithmic Learning in a Random World*. Springer-Verlag, Berlin, Heidelberg, second edition.
- Winters, P. R. (1960). Forecasting sales by exponentially weighted moving averages. *Management Science*, 6(3):324–342.
- Woo, G., Liu, C., Kumar, A., Xiong, C., Savarese, S., and Sahoo, D. (2024). Unified training of universal time series forecasting transformers. *ArXiv*.
- Wood, S. N. (2017). *Generalized Additive Models: An Introduction with R*. Chapman and Hall/CRC, Boca Raton, second edition.
- Yeh, C.-C. M., Fan, Y., Dai, X., Saini, U. S., Lai, V., Aboagye, P. O., Wang, J., Chen, H., Zheng, Y., Zhuang, Z., Wang, L., and Zhang, W. (2024). Rpmixer: Shaking up time series forecasting with random projections for large spatial-temporal data. In *Proceedings of the 30th ACM SIGKDD Conference on Knowledge Discovery and Data Mining*, KDD '24, pages 3919–3930, New York, NY, USA. Association for Computing Machinery.
- Zeng, A., Chen, M., Zhang, L., and Xu, Q. (2023). Are transformers effective for time series forecasting? In *Proceedings of the Thirty-Seventh AAAI Conference on Artificial Intelligence and Thirty-Fifth Conference on Innovative Applications of Artificial Intelligence and Thirteenth Symposium on Educational Advances in Artificial Intelligence*, AAAI'23/IAAI'23/EAAI'23. AAAI Press.

Appendix

A Datasets

Table A1: Dataset Description.

Dataset	Number of Series	Frequency	Mean-Length Series	Lags	Forecast Horizon
Air Passengers	1	<i>monthly</i>	144	12	12
Australian Electricity Demand	5	<i>monthly</i>	159	12	24
Australian Retail Turnover	133	<i>monthly</i>	441	12	24
M3 Monthly	1,428	<i>monthly</i>	117	12	18
M5	70	<i>daily</i>	1,969	14	28
Rossmann Store Sales	1,115	<i>daily</i>	757	21	40
Tourism	366	<i>monthly</i>	299	12	24

B Hyper-Parameters

Table B1: Local Model Hyper-Parameters.

Air Passengers				
Model	Learning Rate	Linear Tree	Epochs	Train Loss
Hyper-Tree-AR	<i>1e-01</i>	<i>True</i>	500	ℓ_2
Hyper-Tree-ES	<i>1e-01</i>	<i>True</i>	500	ℓ_2
LightGBM	<i>1e-01</i>	<i>True</i>	500	ℓ_2
LightGBM-AR	<i>1e-01</i>	<i>True</i>	500	ℓ_2
LightGBM-STL	<i>1e-01</i>	<i>True</i>	500	ℓ_2
Australian Electricity Demand				
Model	Learning Rate	Linear Tree	Epochs	Loss
Hyper-Tree-AR	<i>1e-01</i>	<i>True</i>	500	ℓ_2
Hyper-Tree-ES	<i>1e-01</i>	<i>True</i>	500	ℓ_2
LightGBM	<i>1e-01</i>	<i>True</i>	500	ℓ_2
LightGBM-AR	<i>1e-01</i>	<i>True</i>	500	ℓ_2
LightGBM-STL	<i>1e-01</i>	<i>True</i>	500	ℓ_2
Australian Retail Turnover				
Model	Learning Rate	Linear Tree	Epochs	Loss
Hyper-Tree-AR	<i>1e-01</i>	<i>True</i>	500	ℓ_2
Hyper-Tree-ES	<i>1e-01</i>	<i>True</i>	500	ℓ_2
LightGBM	<i>1e-01</i>	<i>True</i>	500	ℓ_2
LightGBM-AR	<i>1e-01</i>	<i>True</i>	500	ℓ_2
LightGBM-STL	<i>1e-01</i>	<i>True</i>	500	ℓ_2
Tourism				
Model	Learning Rate	Linear Tree	Epochs	Loss
Hyper-Tree-AR	<i>1e-01</i>	<i>True</i>	500	ℓ_2
Hyper-Tree-ES	–	–	–	–
LightGBM	<i>1e-01</i>	<i>True</i>	500	ℓ_2
LightGBM-AR	<i>1e-01</i>	<i>True</i>	500	ℓ_2
LightGBM-STL	<i>1e-01</i>	<i>False</i>	500	ℓ_2

Unlisted hyper-parameters use default values. ℓ_2 denotes MSE-Loss. Entries with “–” indicate non-applicable.

Table B2: Global Model Hyper-Parameters.

Australian Electricity Demand									
Model	Learning Rate	Linear Tree	Epochs	Hidden Layers	Batch Size	# Layers	# Heads	Context Length	Loss
Deep-AR	$1e-03$	–	100	128	128	3	–	2H	NLL
GBM-Net-AR	$1e-01 / 1e-03$	True	100	128	–	–	–	–	ℓ_2
Hyper-Tree-AR	$1e-01$	True	100	–	–	–	–	–	ℓ_2
Hyper-Tree-ES	$1e-01$	True	100	–	–	–	–	–	ℓ_2
LightGBM	$1e-01$	True	100	–	–	–	–	–	ℓ_2
LightGBM-AR	$1e-01$	True	100	–	–	–	–	–	ℓ_2
TFT	$1e-03$	–	100	128	128	–	4	2H	$\tau_{0.5}$
Australian Retail Turnover									
Model	Learning Rate	Linear Tree	Epochs	Hidden Layers	Batch Size	# Layers	# Heads	Context Length	Loss
Deep-AR	$1e-03$	–	500	128	128	3	–	2H	NLL
GBM-Net-AR	$1e-01 / 1e-03$	True	500	128	–	–	–	–	ℓ_2
Hyper-Tree-AR	$1e-01$	True	500	–	–	–	–	–	ℓ_2
Hyper-Tree-ES	$1e-01$	True	500	–	–	–	–	–	ℓ_2
LightGBM	$1e-01$	True	500	–	–	–	–	–	ℓ_2
LightGBM-AR	$1e-01$	True	500	–	–	–	–	–	ℓ_2
TFT	$1e-03$	–	500	128	128	–	4	2H	$\tau_{0.5}$
M3 Monthly									
Model	Learning Rate	Linear Tree	Epochs	Hidden Layers	Batch Size	# Layers	# Heads	Context Length	Loss
Deep-AR	$1e-03$	–	200	128	128	3	–	2H	NLL
GBM-Net-AR	$1e-01 / 1e-03$	True	200	128	–	–	–	–	ℓ_2
Hyper-Tree-AR	$1e-01$	True	200	–	–	–	–	–	ℓ_2
Hyper-Tree-ES	–	–	–	–	–	–	–	–	–
LightGBM	$1e-01$	True	200	–	–	–	–	–	ℓ_2
LightGBM-AR	$1e-01$	True	200	–	–	–	–	–	ℓ_2
TFT	$1e-03$	–	200	128	128	–	4	2H	$\tau_{0.5}$
M5									
Model	Learning Rate	Linear Tree	Epochs	Hidden Layers	Batch Size	# Layers	# Heads	Context Length	Loss
Deep-AR	$1e-03$	–	200	128	128	3	–	2H	NLL
GBM-Net-AR	$1e-02 / 1e-03$	True	200	128	–	–	–	–	ℓ_2
Hyper-Tree-AR	$1e-02$	True	200	–	–	–	–	–	ℓ_2
Hyper-Tree-ES	–	–	–	–	–	–	–	–	–
LightGBM	$1e-01$	True	200	–	–	–	–	–	ℓ_2
LightGBM-AR	$1e-01$	True	200	–	–	–	–	–	ℓ_2
TFT	$1e-03$	–	200	128	128	–	4	2H	$\tau_{0.5}$
Rossmann Store Sales									
Model	Learning Rate	Linear Tree	Epochs	Hidden Layers	Batch Size	# Layers	# Heads	Context Length	Loss
Deep-AR	$1e-03$	–	500	128	128	3	–	2H	NLL
GBM-Net-AR	$1e-02 / 1e-03$	True	500	128	–	–	–	–	ℓ_2
Hyper-Tree-AR	$1e-02$	True	500	–	–	–	–	–	ℓ_2
Hyper-Tree-ES	–	–	–	–	–	–	–	–	–
LightGBM	$1e-02$	True	500	–	–	–	–	–	ℓ_2
LightGBM-AR	$1e-02$	True	500	–	–	–	–	–	ℓ_2
TFT	$1e-03$	–	500	128	128	–	4	2H	$\tau_{0.5}$
Tourism									
Model	Learning Rate	Linear Tree	Epochs	Hidden Layers	Batch Size	# Layers	# Heads	Context Length	Loss
Deep-AR	$1e-03$	–	500	128	128	3	–	2H	NLL
GBM-Net-AR	$1e-01 / 1e-03$	True	500	128	–	–	–	–	ℓ_2
Hyper-Tree-AR	$1e-01$	True	500	–	–	–	–	–	ℓ_2
Hyper-Tree-ES	$1e-01$	True	500	–	–	–	–	–	ℓ_2
LightGBM	$1e-01$	True	500	–	–	–	–	–	ℓ_2
LightGBM-AR	$1e-01$	True	500	–	–	–	–	–	ℓ_2
TFT	$1e-03$	–	500	128	128	–	4	2H	$\tau_{0.5}$

Entries with “–” indicate non-applicable. For GBM-Net-AR, the learning rate shows tree-part / MLP-part. Unlisted hyper-parameters use default values. H : Forecast Horizon, ℓ_2 : MSE-Loss, NLL : Negative log-likelihood of Student-T distribution, $\tau_{0.5}$: quantile loss evaluated at median.

C Example Forecasts

Figure C1: Global Model Forecasts.

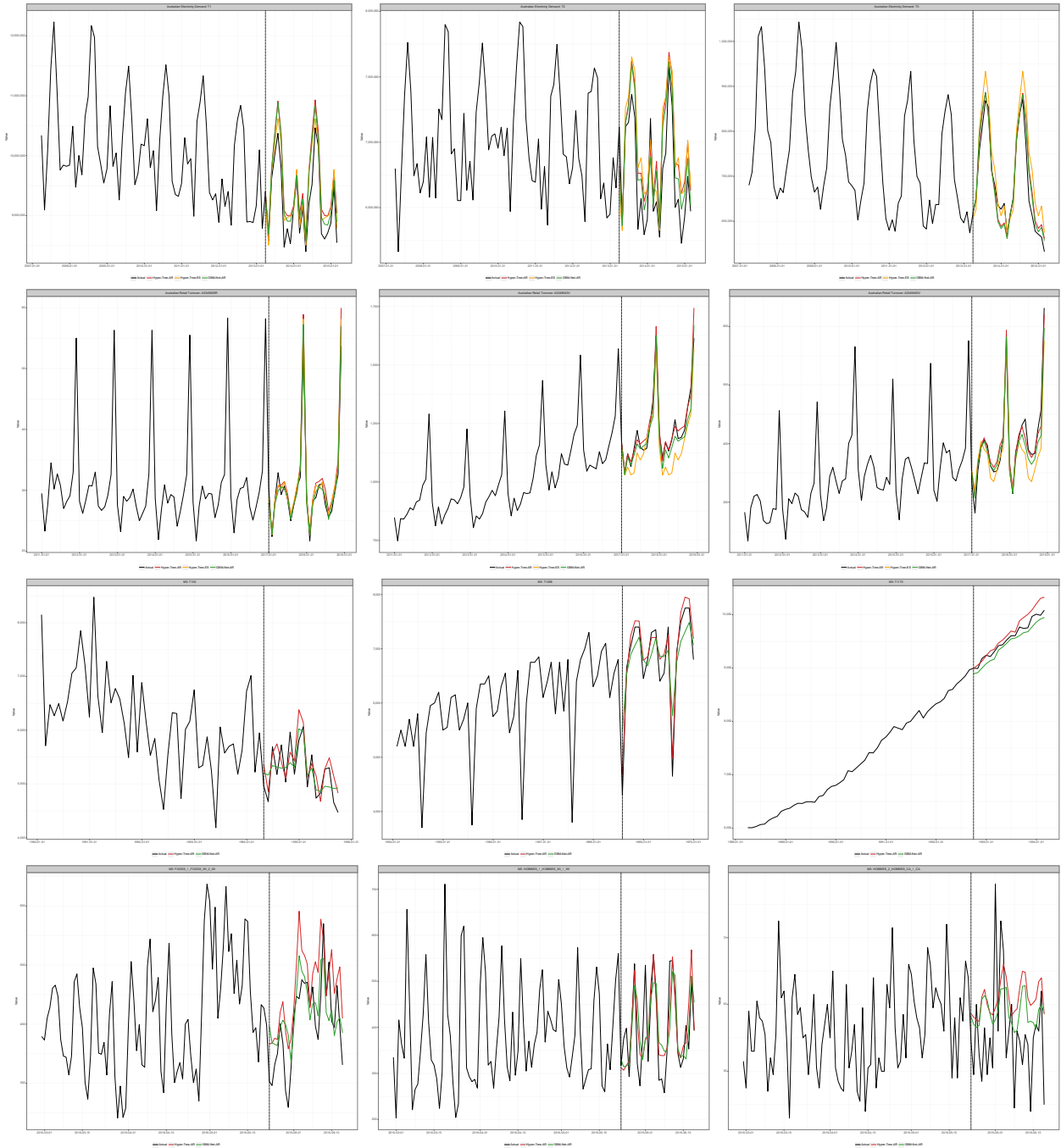


Figure C1: Continued.

